CHALMERS



A combined Li-ion & lead-acid battery system for start-stop application: potential & realization

Authors:
Heza Taha Mahmoud
Lishan Xu

Department of Energy and Environment
Division of Electric Power Engineering and
Department of Materials and Manufacturing Technology
Department of Applied Physics
CHALMERS UNIVERSITY OF TECHNOLOGY
Göteborg, Sweden, Jun 2011

1. Examiner: Torbjörn Thiringer
Department of Energy and Environment
Chalmers University of Technology, 41296 Göteborg, Sweden

2. Examiner: Patrik Johansson
Department of Applied Physics
Chalmers University of Technology, 41296 Göteborg, Sweden

Acknowledgements

This thesis work has been performed at Volvo Cars Corporation in Gothenburg, Sweden. We would like to express our gratitude to people who has been involved to sponsor and help us to complete our work.

We would like to thank our supervisors Daniel Midholm and Torbjörn Larsson for all their help and contributions, which made our work possible to perform.

We would like to thanks our examiners Torbjörn Thiringer and Patrik Johansson, for improving and inspecting the written report.

Moreover, our gratitude goes to people from all the department of power electronic at Volvo, for helping us with the work in the workshop, especially Patrik Larsson, Erik Astlund and Göran Martinsson

We would like to thank Arash Idelchi, who has helped us with the reading of the report and giving us feedback to improve the language of the report.

Finally we would like to thank our families for supporting us with help and understanding.

Abstract

The aim of this master thesis is to investigate the possibility of using lithium-ion batteries as a second battery instead of lead-acid batteries for the start-stop application in vehicles. To achieve the specified target, the following steps are explored: investigation of the technology market, choice of relevant sizing of the battery, development of charge algorithms for the battery system, creation of an electric simulation model with Simulink, development of a prototype for installation in car and finally verification of the new battery model in a vehicle.

The battery which is chosen is a Li-ion battery with a voltage of 16.6V and a capacity of 30Ah due to the test-rig requirements and availability. Before implementation in the vehicle, tests are performed on the battery pack and the combined system. The controller system for charging and discharging is created in Simulink.

Through several experiments, the working voltage range of the Li-ion battery pack was defined from 14.8V to 14.2V. In addition, a verification of this solution has been done in a real vehicle.

Moreover, comparing the experimental results with our literature study, a new type of lithium-ion battery chemistry, which matches the characteristics required in this work is investigated: a $LiFePO_4$ cathode based battery.

Key words: lithium-ion battery, parallel, Simulink. start-stop

Abbreviation List

A	Geometrical area
A	Ampere
ACEA	Association des Constructeurs Européens d'Automobiles
Ah	Ampere hour
A_{in}	Interfacial area
BMS	Battery Management System
C	Capacity of the battery in Ah
CC	Constant Current
C-C bond	Carbon-Carbon bond
Co	Cobalt
CO_2	Carbon Dioxide
Cr	Chromium
C_{usable}	Usable capacity of the battery pack
CV	Constant Voltage
E_{FA}	Fermi Energy of the anode
E_{FC}	Fermi Energy of the cathode
$FePO_4$	Iron phosphate
HEV	Hybrid Electric Vehicle
HOMO	Highest Occupied Molecular Orbital
H_2SO_4	Sulfuric acid
I	Current
Ic_{harge}	Charge Current
$I_{discharge}$	Discharge current
I_{limit}	Current-limit
ICE	Internal Combustion Engine
J	Joule
L	Effective thickness
$LiCoO_2$	Lithium Cobalt Oxide
$LiFePO_4$	Lithium Iron Phosphate
Li-ion	Lithium-ion
$LiPF_6$	Lithium hexafluorophosphate
LUMO	Lowest Unoccupied Molecular Orbital
MABX	MicroAutoBox
Mn	Manganese
Ni	Nickel
Ni-Cd	Nickel Cadmium
NiMH	Nickel Metal Hydride
OCV	Open Circuit Voltage
P	Power
Pb	Metallic lead
PbO_2	Lead dioxide
$PbSO_4$	Lead sulfate
PME	Power Mode Extension
Q_{tot}	Total capacity of the battery pack
R	Resistance
R_c (A)	Internal resistance of the current collector at the anode
R_{cable}	Cable Resistance

R_c (C)	Internal resistance of the current collector at the cathode
R_{cell}	Cell Resistance
R_{el}	Electrolyte resistance
R_{in}	Resistance of the electrolyte-electrode interface
R_{in} (A)	Internal resistance of the anode
R_{inbatt}	Internal resistance of the cell
R_{in} (C)	Internal resistance of the cathode
rpm	Revolutions per minute
s	Second
SEI	Solid Electrolyte Interphase
Si	Silicon
Sn	Tin
SOC	State Of Charge
SOC_{usable}	State Of Charge usable of the battery pack
SOC_{OCV}	State Of Charge depending on OCV
t_{avg}	Average Time
T	Temperature
T_{cell}	Cell Temperature
U	Voltage
V	Volt
V_{cell}	Cell Voltage
W	Watt
$V_{regulator}$	Regulator Voltage
$W_{available}$	Energy Available
W_{losses}	Energy Losses
W_{out}	Energy Output
ΔSOC	Delta State Of Charge
ΔV	Delta Voltage
ΔI	Delta Current
Ω	Ohm
℃	Celsius

Contents

1. Introduction 1
    1.1 Problem background 1
    1.2 Previous work on start-stop application 1
    1.3 The scope of the thesis 3
2. Energy storage 5
    2.1Batteries 5
        2.1.1 Principle of operation 5
    2.2 Different types of rechargeable batteries 6
        2.2.1 Lead-acid batteries 6
        2.2.2 Nickel-Cadmium batteries 8
        2.2.3 Nickel metal hydride batteries 9
        2.2.4 Lithium-ion batteries 9
    2.3 Comparison of different types of batteries and measures 14
        2.3.1 Energy density 14
        2.3.2 Open circuit voltage 14
        2.3.3 Internal resistance 15
        2.3.4 Memory effect 16
        2.3.5 Cycle life 17
        2.3.6 Temperature effects 17
        2.3.7 Cost 18
    2.4 Lithium-ion battery 18
        2.4.1 Cathode materials 19
        2.4.2 Anode materials 21
        2.4.3 Electrolyte materials 21
    2.5 Battery management system (BMS) for Li-ion batteries 22
        2.5.1 Definition of significant parameters in the BMS 22
        2.5.2 Task of the BMS 23
        2.5.3 Design of the BMS 24
    2.6 The final scope of the thesis 25
3. Charge algorithms 26
    3.1 Charge methods for the Li-ion battery 26
    3.2 Charge methods used in the lab 28
4 Tests 29
    4.1 Test setup for lithium ion battery 29
        4.1.1 Charge and discharge tests 30
        4.1.2 Open circuit voltage test 31
    4.2 Proposals of system solutions 31
        4.2.1 System solution A 32
        4.2.2 System solution B 33
        4.2.3 System solution C 34
    4.3 Test performed in vehicles 34
        4.3.1 Electrical management system in the vehicle 35
        4.3.2 Simulink model for calculating SOC and switching relay 35
5. Results and discussion 38
    5.1 Lithium ion battery 38
    5.2 Combined system 44
    5.3 Verification in vehicle 54
6. Conclusions 58

7. Outlook 59
8. References 60

1. Introduction

1.1 Problem background

Due to the regulations established by many legal organizations, the requirement of CO_2 emissions is becoming stricter than before. The ACEA agreement is a voluntary agreement between the European Automobile Manufacturers Association and the European Commission, and it limits the amount of CO_2 emitted by passenger cars, targeting 130g/km by 2015. Therefore, the idea of developing electric vehicles instead of conventional vehicles has become important for the vehicle manufacturers. Due to the feasibility and high cost of electric vehicles, electric vehicles are limited in mass-production market, while hybrid electric vehicles (HEVs) are more popular and commercial.

A HEV combines a conventional internal combustion engine (ICE) propulsion system with an electric propulsion system, and can achieve better fuel economy and lower CO_2 emissions. Some HEVs reduce CO_2 emission at idle state by shutting down the ICE and restarting it when needed. This is considered as a start-stop application, which is investigated in this thesis, with emphasis on the battery providing electrical energy to support the vehicle at idling.

The manufacturers require that the batteries in HEVs provide more energy to decrease fuel consumption of the ICE and that the lifetime of the batteries to be increased. However, the present lead-acid batteries used in the HEVs cannot achieve this goal. To achieve this goal, many investigations about the batteries have been performed all over the world. According to the findings by many research groups, a Li-ion battery is a very promising choice because of its higher energy density, higher OCV (open circuit voltage), lighter weight and other advantages. However, by considering the cost and safety, using lead-acid battery in vehicle applications is still needed to be considered. The main task of this thesis is to investigate how to use a Li-ion battery into the start-stop application in mass production of vehicles.

1.2 Previous work on start-stop application

Figure 1.1 shows the general concept of the battery system in a conventional vehicle. The battery is used to start the engine through a starter. When the engine is running, the alternator is producing power and feeding the loads (the electronic equipment in the vehicle) and charging the battery.

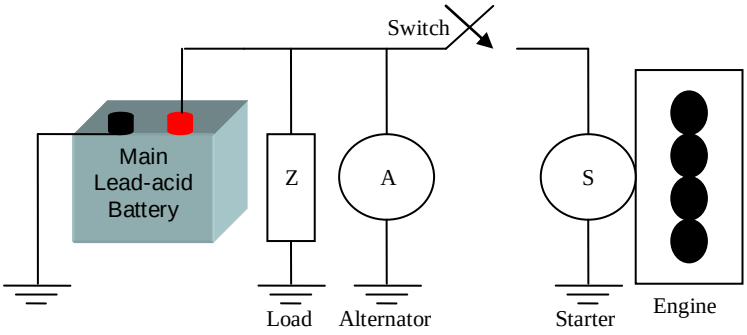


Figure 1.1 An overview of the battery behavior in a conventional vehicle

In so called micro HEVs, a start-stop application has been developed in order to decrease fuel consumption and CO_2 emissions. Instead of one battery, there are two batteries in parallel connected to the electrical system, one with high capacity and the other with lower capacity (Figure 1.2). This is the technology existing in the present vehicles.

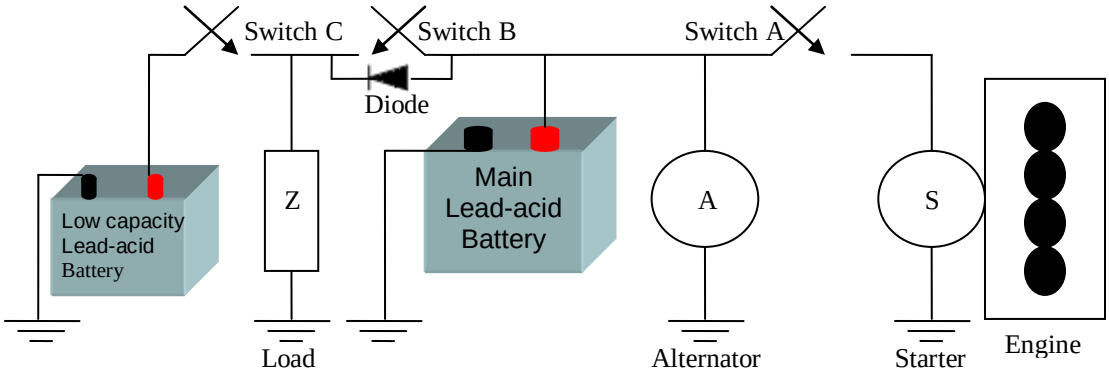


Figure 1.2 Dual battery systems in the start-stop application

Figure 1.3 shows how the switches work in different situations in this dual battery system. Region A is when the vehicle is parking, region B is the time when the vehicle is started and region C happens during stop time.

When the driver cold starts the vehicle, the main lead-acid battery with high capacity will provide the power needed to activate the starter by closing switch A. Then the alternator supplies the power to the loads through switch B is on and charges the main lead-acid battery. When the engine is off during the traffic jam or stops by the purpose of decreasing the fuel consumption and CO_2 emission, only switch B will be activated and the loads will be supported by the main lead-acid battery. Switch C and A are activated during restart the engine again after stop time. So the low capacity battery will support the loads only during a short time until the engine is been started again by the main battery. Then the alternator will charge the dual battery system.

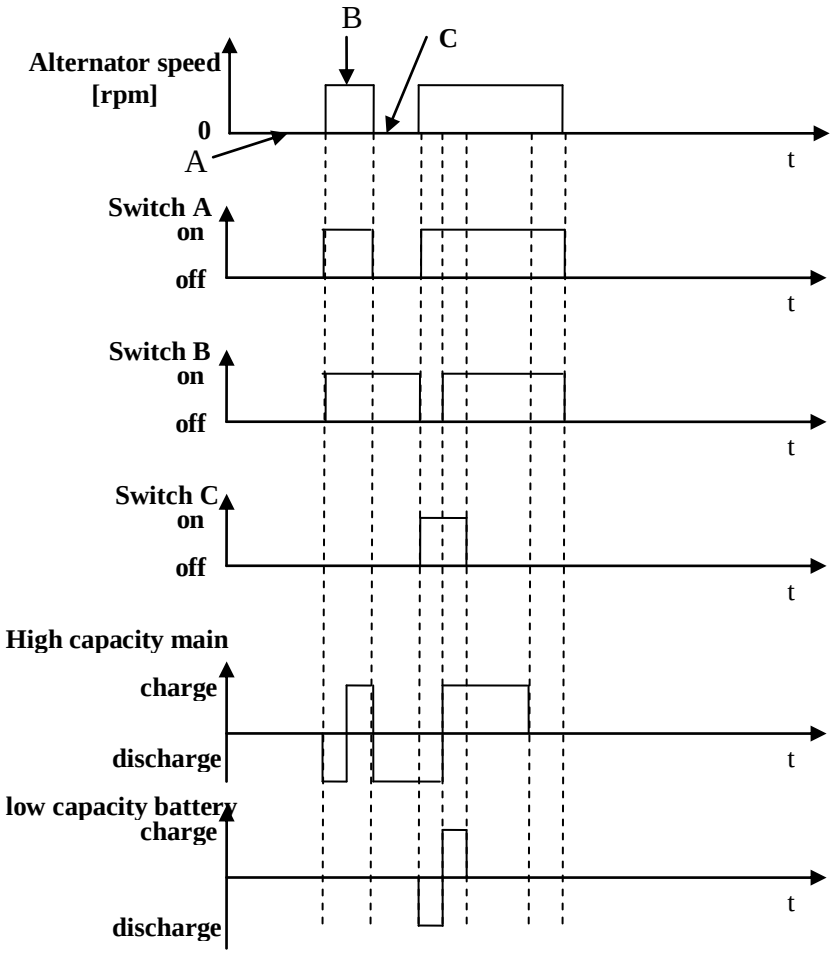


Figure 1.3 Charge and discharge procedure in start-stop application

The start-stop application causes a reduced life time for the lead-acid main battery by the frequent charging processes and high discharge current after the stop function. This phenomenon also influences the lead-acid batteries' own characteristics and eventually does not satisfy the new requirements of the battery system at present (Table 1.1). Therefore, new ideas about energy storage devices in vehicles need to be investigated.

Table 1.1 The new requirements of the battery system

Load current	50A
t_{avg}	20s
Life time	10 years or 3000h
Number of stops	225000
Alternator	13.5-15.2 V & max current out 150A
Lead-acid OCV	12.9V

1.3 The scope of the thesis

According to the new requirements of the battery system, present dual battery system cannot perform so well and a new battery system is needed. From the economic point of view, it would be better to keep the lead-acid main battery because of its lowest price

among all the batteries. Due to the safety and convenience reason, lead-acid battery has very great stability to provide high current to activate the engine. Basing on these ideas, the low capacity lead-acid battery will be replaced by a new type battery.

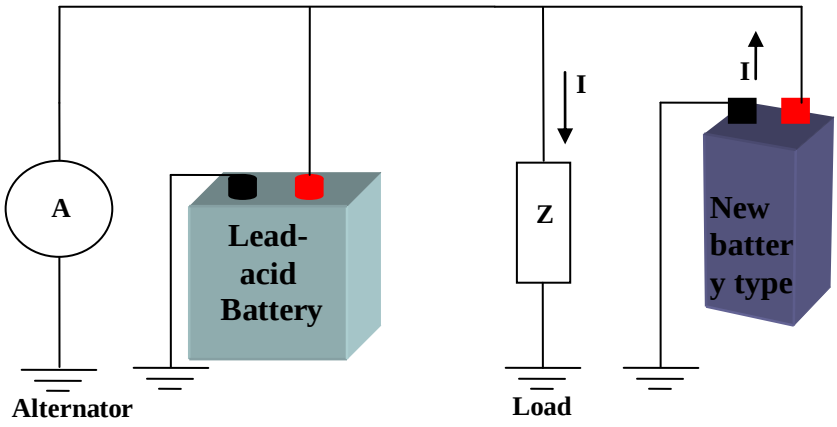


Figure 1.4 Improvement of the start-stop application in vehicles

Figure 1.4 shows one idea of how a system may be designed to improve the start-stop application during the stop time. It depicts the parallel connection between the new battery type (the second battery) and the lead-acid battery. In this scope, the lead-acid battery will activate the engine and the alternator will supply the power to the loads during driving time. Due to using the second battery, the loads will be supported during the stop time until the alternator works. The alternator will recharge both batteries when the engine re-starts. The scope will increase the life time of the battery system by reducing the usage of the main lead-acid battery, which is a significant aspect in the new requirements.

2. Energy storage

In order to investigate a new battery type, a detailed understanding of battery knowledge is required.

2.1Batteries

Batteries are energy storage devices which convert chemical energy to electrical energy. Strictly speaking, batteries are comprised of several electrochemical cells and each cell mainly contains a negative electrode (anode), a positive electrode (cathode), and an electrolyte (Figure 2.1). The electrolyte conducts ions and insulates vs. electrons; each electrode is connected to a current collector which assures the electrons to flow into the external circuit. If the electrolyte is liquid, a separator must be added to keep the electrodes apart, while if the electrolyte is solid, it acts as a separator. At the anode, M is oxidized, it loses one electron and becomes M^+ cation, and then the electrons flow through the external circuit. Meanwhile, X is reduced at the cathode, it achieves one electron from the anode through external circuit and become X - anion. In this way, current is produced.

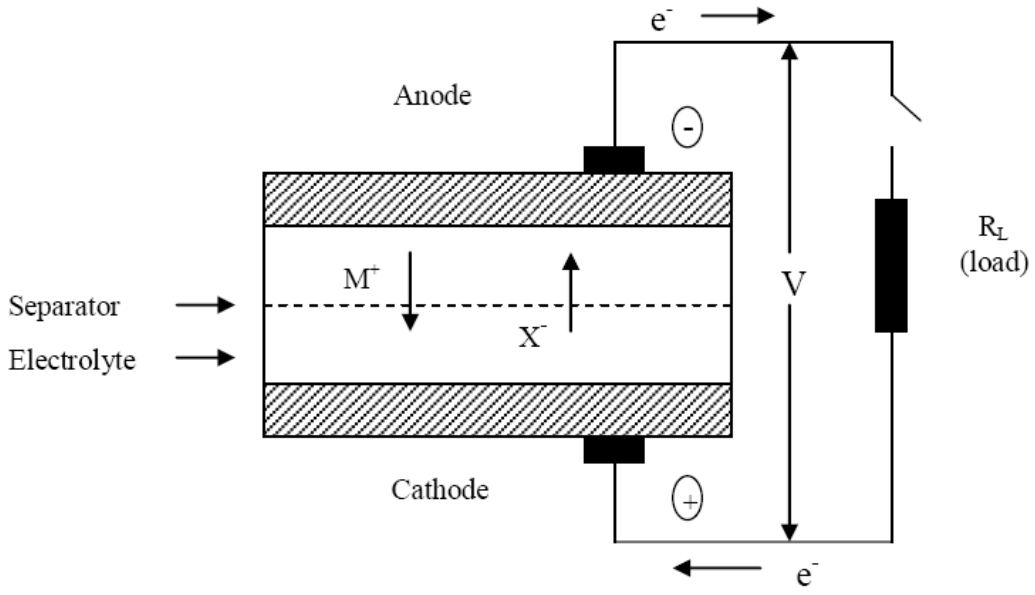


Figure 2.1 Sketch of components of a cell with current flows during discharge

2.1.1 Principle of operation

It is the redox reactions occurring inside the battery that produce the electrical energy. The driving force for the reactions is Gibbs free energy, which can be achieved by the thermodynamic formulation. The basic thermodynamic equation for a reversible electrochemical reaction is given as followed:

$$\Delta G = \Delta H - T\Delta S \qquad (2\text{-}1)$$

ΔG is the Gibbs free energy or the energy that can be provided for useful work. ΔH is the enthalpy, which is the entire energy released by the reactions. ΔS is the entropy, and T is the absolute temperature, while TΔS represents the heat dissipation with random movement of materials.

Since ΔG represents the net useful work energy available from the reactions, the net available electrical energy from the reactions can be given by the following formula:

$$E = -\Delta G / nF \quad (2\text{-}2)$$

Where E is the cell voltage, n is the number of electrons transferred per mole of reactant, and F is the Faraday constant (96486 Coulombs/mole) [2].

2.2 Different types of rechargeable batteries

Several types of rechargeable batteries are utilized in the vehicle market. They can be categorized based on the type of electrolyte they use: aqueous, organic solvent, polymer, ceramic etc. By considering the popularity and significance of the batteries used in the vehicle mass-production, four types of batteries are described here: lead-acid batteries, Nickel-Cadmium batteries, nickel metal hydride batteries and Li-ion batteries.

2.2.1 Lead-acid batteries

The lead-acid battery was the first rechargeable battery developed, and has been used for nearly 140 years. Lead dioxide (PbO_2) is the positive electrode, metallic lead (Pb) is the negative electrode, and the electrolyte is sulfuric acid (H_2SO_4). Two common types of lead-acid batteries are utilized in the market: one is flooded lead-acid battery and another is valve-regulated lead-acid battery. Due to the need of low cost batteries in the industry, flooded lead-acid battery is the preferred one between these two, which is also used in the experiments in this thesis.

During the discharge process, the following half equation takes place at the negative electrode (anode):

$$Pb + HSO_4^- \rightarrow PbSO_4 + H^+ + 2e^- \quad (2\text{-}3)$$

Metallic lead reacts with H_2SO_4 to form a non-conductive solid product of lead sulfate, $PbSO_4$. Metallic lead loses electrons and becomes lead cations in the above reaction and in the charge process, the reaction is reversible.

Meanwhile, the other half reaction happens at the positive electrode, the reaction is as follows:

$$PbO_2 + 3H^+ + HSO_4^- + 2e^- \rightarrow PbSO_4 + 2H_2O \quad (2\text{-}4)$$

This reaction is also reversible.

According to the two half reactions above, the total reaction equation is:

$$Pb + PbO_2 + 2H_2SO_4 \underset{charge}{\overset{discharge}{\rightleftharpoons}} 2PbSO_4 + 2H_2O \quad (2\text{-}5)$$

In the ideal case, the discharge capacity should stay constant after cycling of the cell. However, during the cycling process, a number of processes degrade the battery and limit the performance. Flooded lead-acid batteries suffer from one or more of the following mechanisms [3]:

A Positive-plane expansion

$PbSO_4$ has a totally different morphology and crystal structure compared to PbO_2. As shown in Figure 2.2, $PbSO_4$ occupies larger volume than PbO_2. In repetitive charge processes, PbO_2 can be re-deposited, but not within original volume. With continuous cycling, this may cause expansion of positive active mass. The expansion of negative plate does not show the same tendency, because Pb is softer than PbO_2 and therefore the active mass is easier to compress to tolerate the expanded volume. Progressive expansion of the positive active mass leads to loss of coherence to the grid, which is a dominant factor related to cycling life.

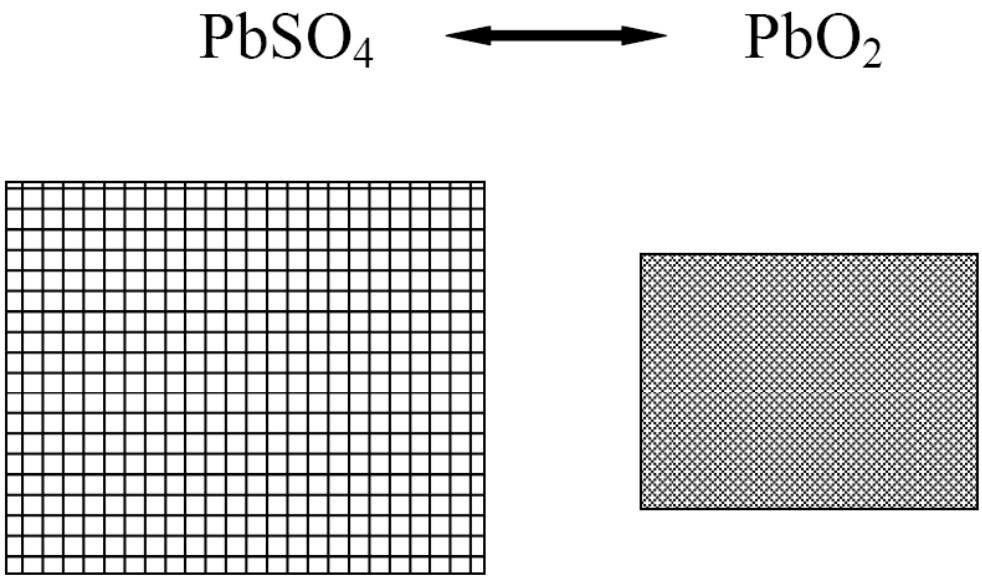


Figure 2.2 Volumes of PbSO4 and PbO2, each has the same amount of lead atoms

B Water loss

Electrolysis of water evolves oxygen at the positive plate and hydrogen at the negative plate. It does not only occur during charge and overcharge processes, but also during the open circuit conditions at low rate like self-discharge. Production of hydrogen and oxygen reduce the volume of the electrolyte so that some of the active mass loses contact with the liquid electrolyte. This process can increase the internal resistance, which, in turn, can cause excessive heat during recharging and consequently fast water loss.

C Acid stratification

While recharging occurs, H_2SO_4 is formed in the porous structure of the active mass. The density of this new formed H_2SO_4 is higher than that of the electrolyte [4]. Hence, the high-density H_2SO_4 would sink down to the bottom of the cell due to the gravity, which can be depicted in Figure 2.3. The acid density is not homogeneous anymore. There is a gradient of acid density- high density at the bottom of the cell while low density at the top of the cell. This effect is called acid stratification. This effect can give rise to the non-uniform utilization of the active mass and, consequently, shorten the service life of the battery.

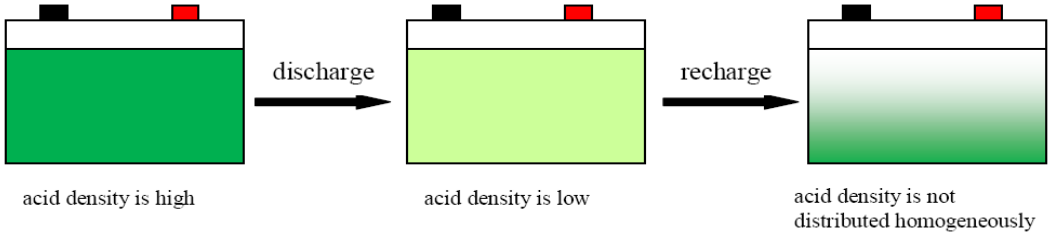


Figure 2.3 Distributions of acid densities in lead-acid battery

D Sulfation

The phenomenon called sulfation is a major aging factor. The active mass reacts with H_2SO_4 to form $PbSO_4$, $PbSO_4$ firstly forms in a finely amorphous state and easily to convert to the active mass reversibly. After repetitive charge and discharge processes, $PbSO_4$ slowly converts to a stable crystalline form that no longer dissolves. Highly crystalline $PbSO_4$ forms at the plates and cannot convert to the active form irreversibly, resulting in a corresponding loss of capacity.

E Corrosion

Positive grid corrosion is still the most frequent cause of lead-acid battery failure. Metallic lead in the positive plate is unstable and the corrosion is unavoidable. Fortunately, the formed corrosion film can protect the metallic substrate, so the corrosion process becomes slow. In some cases, $PbSO_4$ would be formed in the corrosion layer and lead to the mechanical stress, causing the formation of cracks.

2.2.2 Nickel-Cadmium batteries

Alkaline electrolyte batteries have the energy density which is double than that of lead-acid batteries. Perhaps the most common alkaline electrolyte battery in the market is nickel cadmium batteries.

In Ni-Cd batteries, nickel hydroxide $Ni(OH)_2$ is used as the positive electrode, cadmium as the negative electrode and potassium hydroxide KOH as the electrolyte.

At the positive electrode, the reaction equilibrium equation can be exhibited as follows [5]:

$$2NiOOH + 2H_2O + 2e^- \underset{charge}{\overset{discharge}{\rightleftharpoons}} 2Ni(OH)_2 + 2OH^- \quad (2\text{-}6)$$

The half-cell reaction occurring at the negative electrode:

$$Cd + 2OH^- \underset{charge}{\overset{discharge}{\rightleftharpoons}} Cd(OH)_2 + 2e^- \quad (2\text{-}7)$$

The total reaction can be described in the following formula:

$$2NiOOH + Cd + 2H_2O \underset{charge}{\overset{discharge}{\rightleftharpoons}} Ni(OH)_2 + Cd(OH)_2 \quad (2\text{-}8)$$

2.2.3 Nickel metal hydride batteries

Nickel metal hydride batteries are related to nickel cadmium batteries and only use hydrogen-absorbing negative electrode instead of cadmium negative electrode. Therefore, the reaction at the positive electrode is the same as in (2-6).

The half-cell reaction at the negative electrode is as follows [5]:

$$H_2 + 2OH^- \underset{charge}{\overset{discharge}{\rightleftharpoons}} 2H_2O + 2e^- \quad (2\text{-}9)$$

Therefore, the total reaction is:

$$2NiOOH + H_2 \underset{charge}{\overset{discharge}{\rightleftharpoons}} 2Ni(OH)_2 \quad (2\text{-}10)$$

2.2.4 Lithium-ion batteries

Lithium is the lightest metal and has a high electrochemical potential. These properties enable lithium metal to achieve high energy and power density and become a promising material in the battery production market.

Rather than only using the redox reaction as in the above three types of batteries, Li-ion batteries also depend on intercalation. Lithium ions are inserted into the lattice of the host electrode without changing the crystal structure. The principle of Li-ion batteries is shown in Figure 2.4.

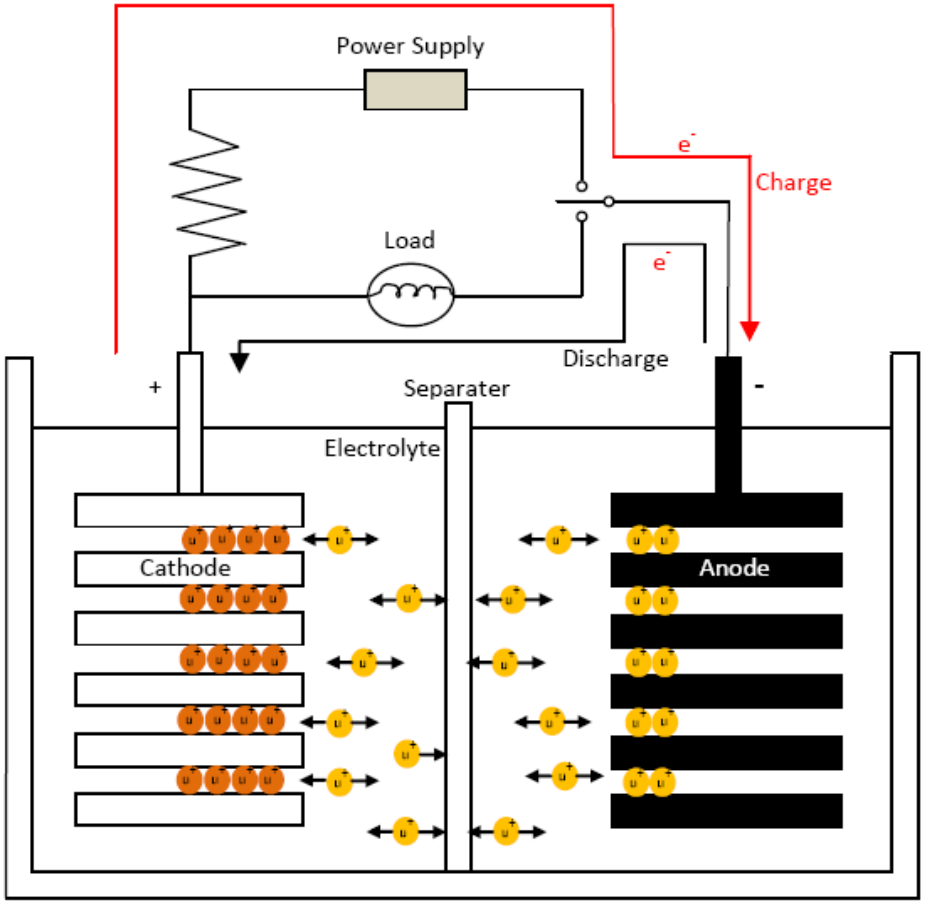


Figure 2.4 The principle of lithium-ion battery

In a typical Li-ion battery, the anode is carbon (graphite), while the cathode is made from lithium cobalt dioxide ($LiCoO_2$) and the electrolyte is a non-aqueous organic solvent including a lithium salt ($LiPF_6$).

The half-cell reaction at the positive electrode is:

$$xLi^+ + xe^- + Li_{1-x}CoO_2 \underset{charge}{\overset{discharge}{\rightleftharpoons}} LiCoO_2 \tag{2-11}$$

The reaction at negative electrode is as follows:

$$Li_xC \underset{charge}{\overset{discharge}{\rightleftharpoons}} xLi^+ + xe^- + C \tag{2-12}$$

In sum, the total reaction is

$$Li_{1-x}CoO_2 + Li_xC \underset{charge}{\overset{discharge}{\rightleftharpoons}} LiCoO_2 + C \tag{2-13}$$

During discharge, lithium ions are dissociated, migrate across the electrolyte and are inserted into the carbon structure. At the same time the compensating electrons flow in the external circuit. Because this reaction is reversible, the lithium ions pass back and forth between the electrodes during charging and discharging.

Li-ion batteries also suffer from aging mechanisms, which increase the internal resistance, induce the capacity loss and shorten the cycle life. Unfortunately, Li-ion batteries are a complex system to understand and the aging mechanisms inside this type are more complicated to describe. Therefore, in this paper, an attempt is made to try to identify and explain the mechanisms of aging in Li-ion batteries from many literature papers.

Aging mechanisms occurring at the different components inside Li-ion batteries (e.g. the anode, and the cathode) have different principles, so they will be discussed separately [6].

A. Aging at the anode

Carbon, especially graphite, is the most popular anode material in Li-ion batteries, and is also the anode material of Li-ion batteries used in this case. Aging mechanisms occurring at the anode are caused by three different changes (1) changes at the anode/electrolyte interface, (2) changes of the active material, and (3) changes of the composite electrode. Many research groups consider that changes at the anode/electrolyte interface is the dominating aging mechanism at the anode, and the other two changes are seldom discussed; however, they really influence the aging mechanisms, which will be described shortly later.

1. Changes at the anode/electrolyte interface

The electrolyte decomposes and reacts with the carbon anode during the initial charge, thus forming protective layers covering the surface. At some graphite sites, Li-ions migrate into/out of the host's crystal structure. Therefore, the thin passivating layers formed here are called SEI layers (solid electrolyte interphase). These SEI layers protect (1) the electrolyte from further reduction, and (2) the charged electrode from corrosion.

Usually, SEI formation is accompanied by the emission of gas electrolyte decomposition products in the first few cycles. The irreversible capacity loss happens during SEI formation. In the later cycling, due to self-discharge, the corrosion of the anode and the electrolyte decomposition are ongoing; however, compared to the first cycle, the rate is lower. During a long time, SEI penetrates into the pores of the electrodes and results in a decrease of accessible active surface area of the anode, which increase the internal resistance. Some studies reveal that exothermic side reactions of lithiated carbon can cause self-heating. Elevated temperature cause a dramatic influence on SEI degradation. The SEI layers start to dissolve and a re-precipitation of dissolve SEI may take place. In this way, meta-stable organic SEI layers will convert into stable inorganic products, which results in a lower ionic conductivity of the SEI layers for lithium.

Low temperature also causes many problems. Due to low temperature, the kinetics of lithium insertion and extraction are very slow, and these effects are very pronounced at low temperature. Metallic lithium plating and lithium dendrite formation are considered

as parasitic side reactions during the charge process. These phenomena induce aging. All the aging mechanisms described here can be seen in Figure 2.5.

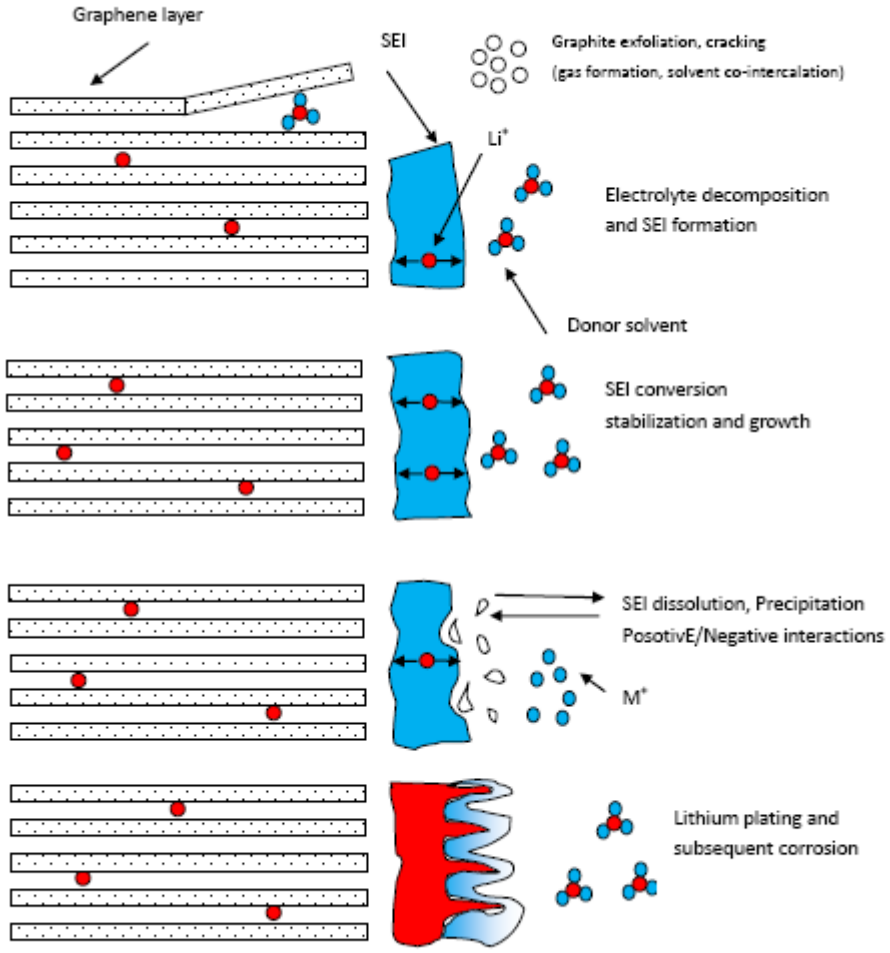


Figure 2.5 Change at the anode/electrolyte interface

2. Changes of the active material

Within the active material, only minor aging effects have been explored. The volume changes of graphite during the insertion and extraction of lithium ions can cause mechanical stress on defects and C-C bonds, which may lead to crack or structural damage. The degradations of the electrodes discussed before have a strong impact on the changes of active material.

3. Changes of the composite electrodes

Generally, the contact-loss within the electrodes results in the increasing internal resistance and is considered as the reason for aging. One resource of contact-loss is the volume change discussed before.

In sum, changes at the anode/electrolyte are the main aging mechanism occurring at the anode. SEI formation and conversion cause the increased internal resistance and capacity-loss in the battery. The volume changes of the active material lead to crack and

structural damage and also induce the contact loss within the anode, which increases the internal resistance in the anode.

B. Changes at the cathode

The aging at the cathode material also affects the performance, as well as the cycling life and capacity loss. In this part, some basic aging mechanisms will be summarized. The mechanisms of capacity-loss are not completely understood at the moment. The changes occurring at the cathode having an influence on the cycling life of Li-ion batteries are categorized as followed.

- Changes of the active material
- Degradation of the electrode components including the binder, the current collector
- Decomposition of the electrolyte and surface film formation
- Insertion of aging products into the anode

These effects cannot happen separately and are influenced by each other. The vivid description of the aging mechanisms can be shown clearly in Figure 2.6.

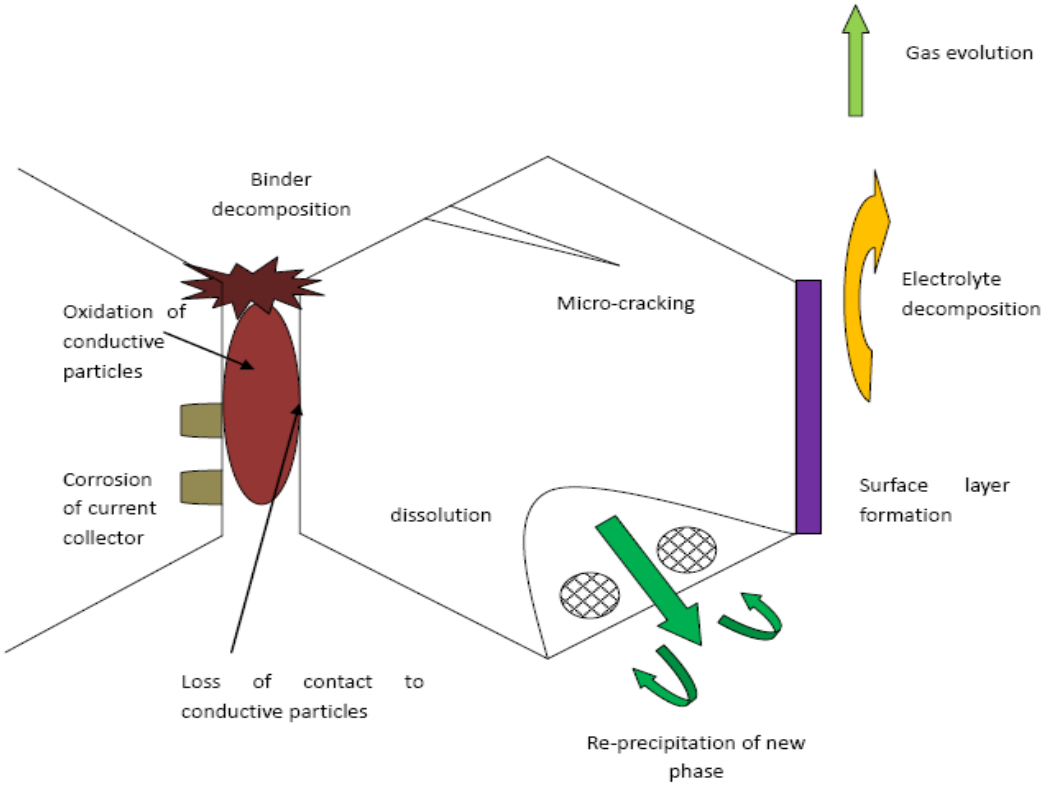


Figure 2.6 Changes at the cathode

In sum, although the aging mechanisms occurring in the Li-ion batteries are not understood clearly at present, some basic mechanisms are described in this chapter. Battery aging mechanisms influence the internal resistance, cycling life and capacity-loss obviously. Due to the cell chemistry, the state of charge deteriorates the characteristics of the Li-ion batteries. High temperature accelerates the aging, while, low temperature also have a negative impact on the performance. Surface chemistry, phase transitions and volume changes would take main responsibility for the aging in the Li-ion batteries.

2.3 Comparison of different types of batteries and measures

2.3.1 Energy density

Energy density is the energy storage per unit weight or per unit volume in the battery. The comparison of energy density in these four popular batteries can be observed clearly in Figure 2.7. Lithium-ion batteries have the best energy density not only per unit weight but also per unit volume. Lead-acid batteries have the lowest.

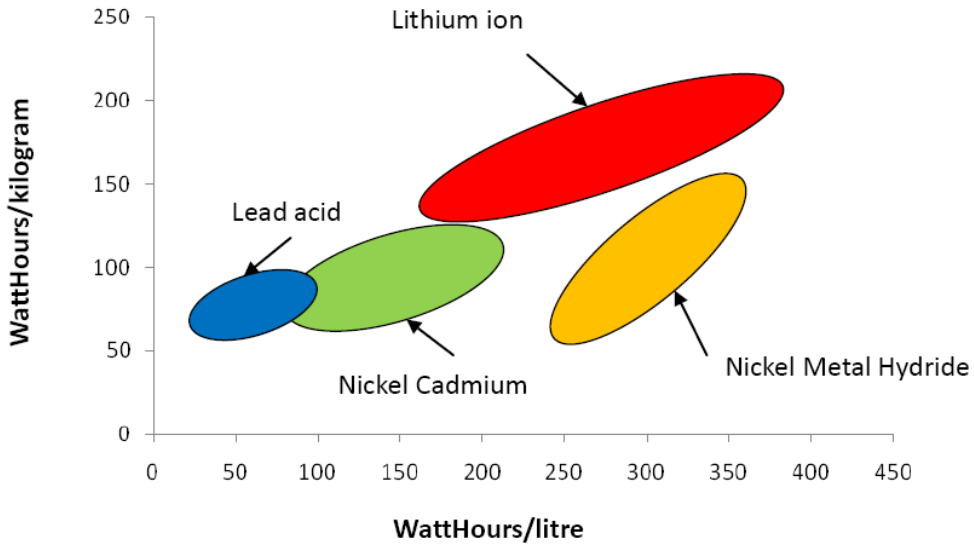


Figure 2.7 Comparison of energy density for different types of batteries

2.3.2 Open circuit voltage

In order to increase the energy density of a cell, it is necessary to increase the voltage. The voltage provided by the cell is [1]

$$V = V_{OCV} - I\,R_{inbatt} \tag{2-14}$$

V_{OCV} is the open circuit voltage and IR_{inbatt} is the voltage loss due to the internal resistance R_{inbatt} of the cell. In order to increase the voltage V, the internal resistance R_{inbatt} should be minimized and the OCV maximized. V_{OCV} is given as followed

$$V_{OCV} = (E_{FA} - E_{FC}) / e \tag{2-15}$$

V_{OCV} is expressed by the difference of the Fermi energies, which are the electrochemical potentials of the two electrodes, and e is the charge delivered by the electron. More details can be observed in Figure 2.8. To achieve the thermodynamic stability, the anode Fermi energy E_{FA} must lie below the lowest unoccupied molecular

orbital (LUMO) of the electrolyte. Accordingly, the cathode Fermi energy E_{FC} should lie above the highest occupied molecular orbital (HOMO) of the electrolyte. To increase the OCV of the cell, a non-aqueous electrolyte with a wide stability window is necessary.

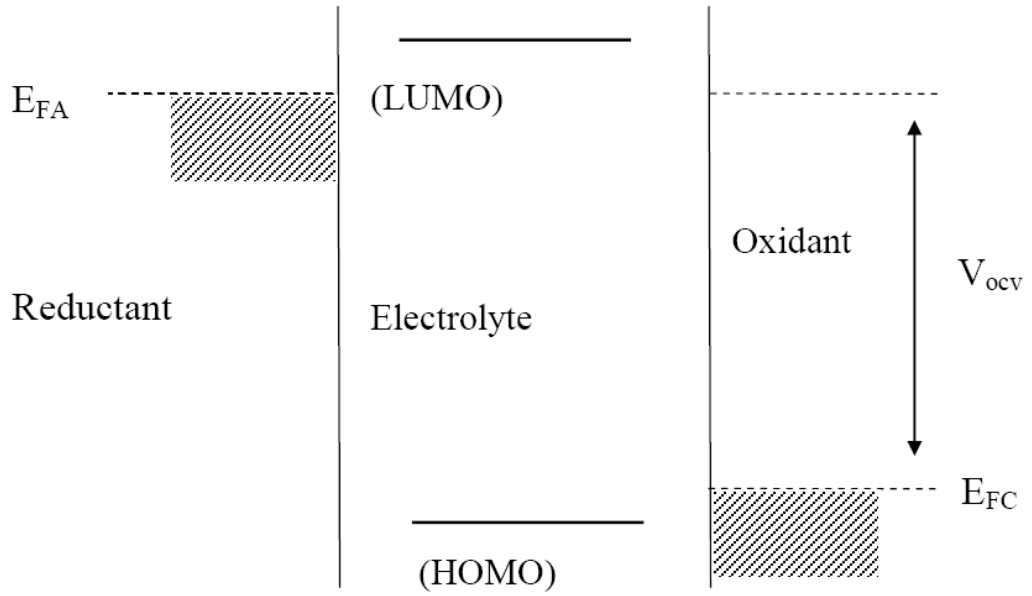


Figure 2.8 The role of Fermi energy for the two electrodes and LUMO and HOMO for the electrolyte to achieve a stable battery

Only Li-ion batteries, with their possibility of a very large OCV, use a non-aqueous electrolyte.

2.3.3 Internal resistance

Internal resistance is also a main factor that affects the voltage as well as the thermal management and the cycle life of the cell [8].

Generally, the internal resistance of the whole cell can be expressed as followed.

$$R_{inbatt} = R_{el} + R_{in}(A) + R_{in}(C) + R_c(A) + R_c(C) \quad (2\text{-}16)$$

The internal resistance of the electrolyte plays an important role in the calculation of the cell's internal resistance, so it is significant to understand which factors influence the internal resistance of the electrolyte.

The electrolyte resistance

$$R_{el} = L/(\sigma i * A) \quad (2\text{-}17)$$

is proportional to the effective thickness L and inversely proportional to the geometrical area A of the inter-electrode space and the ionic conductivity of the electrolyte σi. σi is up to 0.1 S•cm $^{-1}$ [8]. In order to get minimum electrolyte resistance, large geometrical area and short effective thickness are required.

The resistance of the electrolyte-electrode interface is proportional to the ratio of the geometrical area A and the interfacial area A_{in} at each electrode.

$$R_{in} \sim A/A_{in} \tag{2-18}$$

The areas are relevant to the structure inside the cell and the aging mechanisms occuring inside; that is, they would change frequently, especially at the initial cycling.

The current collector resistance R_c of each electrode is related as follows:

$$R_c = (l/(A * \sigma e)) + (1/(d * \sigma m) \tag{2-19}$$

In equation 2-19, l is the mean distance an electron travels through the thickness of the electrode and σe is the electronic conductivity, while σm is the conductivity of the current collector and d is a geometrical parameter having units of length.

Actually, according to the reactions and aging mechanisms inside the cell, and are difficult to identify theoretically. However, some values from the experiments from the other research groups can show that the internal resistance of lead-acid batteries would be the lowest by comparing with the others [9].

2.3.4 Memory effect

Memory effect describes the situation in which the batteries gradually lose their capacity after repeated recharge after being partially discharged. The batteries appear to remember the smaller capacity. Actually, this effect only occurs inside the nickel-based batteries due to the specific phase occurring in this type battery and it is the major reason why the nickel based batteries are rarely used in the market [10].

The cause of memory effect is reported to be due to the formation of γ-NiOOH by overcharging [10]. Figure 2.9 depicts the overall reactions and phase transformations happening during charge and discharges of the positive electrode:

During the charge process, β-Ni $(OH)_2$ is changed into β-NiOOH with a 15% volume decrease, then when it comes to overcharge, γ-NiOOH is formed with a 44% volume increase. Discharging of γ-NiOOH occurs normally by producing an intermediate phase, α-Ni $(OH)_2$, reversely, charging of α- Ni $(OH)_2$ could also produce γ-NiOOH. Therefore, γ-NiOOH is very common to occur inside the cell, especially in the initial cycling. If γ-NiOOH exists in the cell, the memory effect would affect the properties of the nickel based batteries.

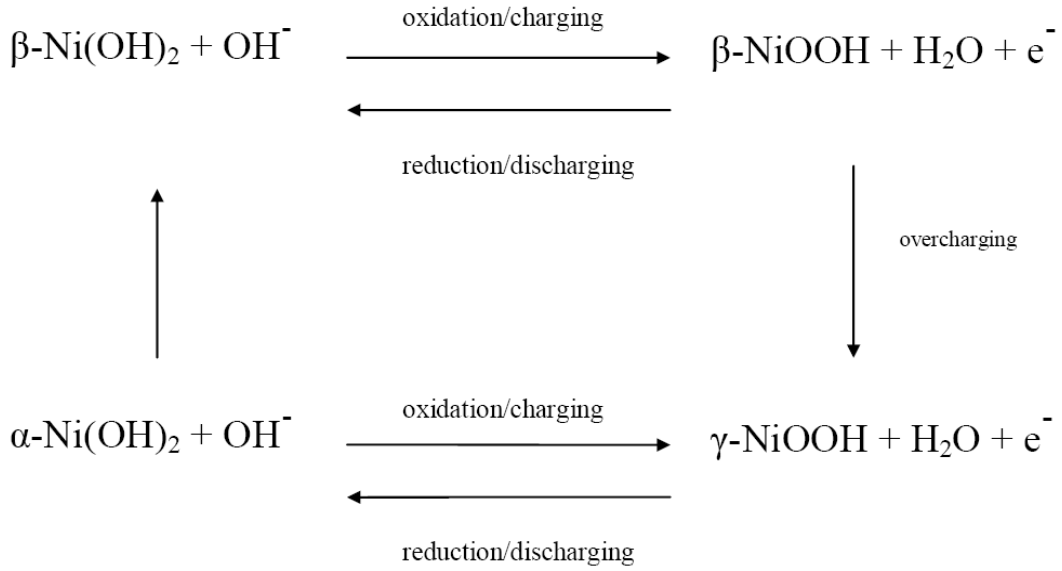


Figure 2.9 Phase transformation inside nickel-based batteries

2.3.5 Cycle life

The definition of cycle life is the number of complete charge-discharge processes performed by a battery; when the capacity drops to 80% of the initial rated capacity, the life of this battery is over. Usually, the aging mechanisms result in capacity loss after repeated recharge, which influence the cycle life obviously. When a battery reaches its cycle life, it will not stop working suddenly. Typical cycle life can be observed in Table 2.1 [12].

Table 2.1 Cycle time of different types of batteries

Types	Lead-acid	Nickel cadmium	Nickel metal hydride	Lithium-ion
Cycle life	300~500	Over 500	500	1000~3000

2.3.6 Temperature effects

High temperatures can accelerate the rate of the chemical reactions and increase the performance of the battery. Meanwhile, the rate of undesirable chemical reactions will increase and induce the loss of cycle life. If the heat generated in the battery exceeds the heat transferred to the ambient environment, the temperature of the battery will continue to rise and result in disastrous damage to the battery [13].

In the low temperature situation, when the temperature reaches the freezing point of the electrolyte inside the battery, the battery is nearly out of work. When below the freezing point of the electrolyte, the battery performance deteriorates as the rates of the chemical reactions are reduced.

Among these four types of batteries, from theoretical data, they nearly have the similar temperature range; relatively the performance of lead-acid batteries owns the priority in reality. At the high temperature, for the sake of achieving the same capacity, generally the volume and size of lead-acid battery is much larger than the other three batteries, so the lead-acid battery has larger surface area to release the heat trapped inside the battery. In this way, the temperature would not increase so quickly to damage the battery.

At the low temperature, comparing lead-acid battery with Li-ion battery, the freezing point of the lead-acid battery is lower than that of the Li-ion battery, so when decreasing the temperature, the Li-ion battery is easier to transfer into the solid and impede the ion diffusion mechanism. If the judgment of temperature can be defined in the research lab, it does not work in application, especially the vehicle industry which requires knowledge of long-term effects. Therefore, BMS (battery management system) which will protect the battery to be damaged by the temperature is required (more details will be explained in the following part).

2.3.7 Cost

According to Table 2.2, the cost of flooded lead-acid battery is the lowest, which is also the sample used in the lab. From this point, it is not economical to utilize any other battery to replace the flooded lead-acid battery in the vehicles, especially in the mass-production vehicles. This aspect is a subtle advantage for lead-acid batteries. However, the capacity of Li-ion batteries required in this thesis is around 30Ah, so the cost of Li-ion batteries is about 100 dollars. This can be accepted if the Li-ion batteries can increase the life time of the battery system as expected.

Table 2.2 Cost for different types of batteries

	Flooded lead aicd	Ni-MH	Lithium-ion
Energy requirement (Wh)	800	800	800
Specific energy (Wh kg^{-1})	30	55	90
Mass (kg)	26.7	14.5	8.9
Mass reduction (kg)	basis	-12.1	-17.8
Example cost (US $)	25	500	300
Cost increase (US $)	basis	475	275

2.4 Lithium-ion battery

The cathode, the anode and the electrolyte are the main important components inside the Li-ion battery. Their specifics will be explained briefly below.

2.4.1 Cathode materials

The lithium-ion battery is the most promising rechargeable battery at present. It has higher energy density, higher OCV, and lighter weight. This part will mainly discuss three common types of lithium-ion batteries based on the cathode materials: $LiMO_2$ (M = Cr, Co, Ni, Mn etc), $Li_xMn_yO_{1-x-y}$ and $LiFePO_4$ [1].

A. Layered $LiMO_2$ cathodes

Li^+ and M^{3+} ions can be ordered into alternate (111) octahedral-site plane of a face center cubic (FCC) of oxide ions (Figure 2.11). This structure has strong layers of edge-shared (MO_2^-) octahedral that are bound to one another by lithium ion in the intervening octahedral-site plane. The extraction of lithium ions proceeds from the space between the layers normally if Li^+ and M^{3+} ions are well ordered. However, when the removal of lithium excesses a critical fraction of lithium inside this structure $LiMO_2$, the $Li_{1-x}MO_2$ phase becomes meta-stable and the electrical force will drive the M cations into the lithium planes. If they have a strong octahedral-site structure, the meta-stable MO_2 layers can be retained until the removal of all the lithium ions.

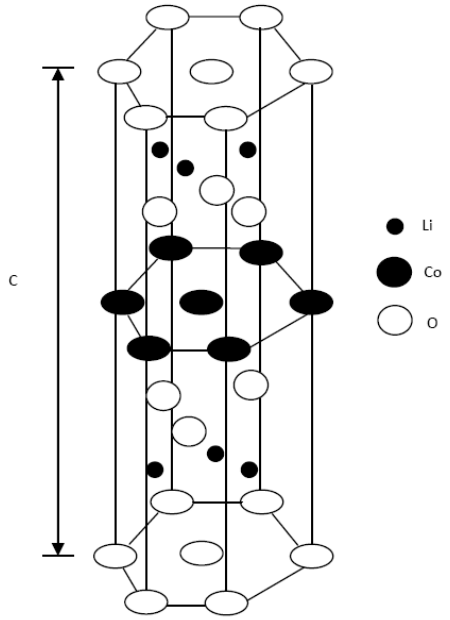


Figure 2.11 Structure of LiCoO2

Cr, Co, Ni, Fe and Mn metals match the profiles, which require the structures have a strong octahedral-site structure and M^{4+}/M^{3+} redox couple inside at a low energy to get a high OCV. The Fe^{3+} ions do not have strong octahedral-site structure and two Mn^{3+} ions are easy to be transferred into Mn^{4+} and Mn^{2+} and Mn^{2+} has no octahedral-site structure. Moreover, Cr^{4+} ions undergo the side reaction and produce the Cr^{6+} ions to occupy the tetrahedral places to block lithium-ions diffusion.

Therefore, the most suitable M^{3+} ions are Co^{3+} and Ni^{3+}. However, partial transition of Ni^{3+} to Ni^{2+} induce that it is difficult to synthesize well-ordered lithium nickel oxide. So, perhaps Co^{3+} would be the most commercial choice.

In sum, the layered $LiMO_2$ cathode materials offer the high energy density as well as a large capacity due to its structure. However, by considering the high cost and toxicity of

cobalt, they are of good use in low power applications. When it comes to the high power applications, the layered $LiMO_2$ cathode materials are limited by the high internal temperature produced, in addition to the high expense. Because the metastable hosts inside the layered $LiMO_2$ cathode materials can be disordered by the high temperature. The 3D framework oxides discussed below are more competitive for power applications in the vehicles where multiple cells are required and high internal temperature can be avoided.

B. Spinel framework $Li_xMn_yO_{1-x-y}$ cathodes

In Figure 2.12, the $A(M_2)O_4$ ideal cubic spinel structure contains A cations at 8a tetrahedral sites and M cations at 16d octahedral sites, oxygen atoms occupying 32e sites and vacancy at 16c sites. The $(M_2)O_4$ array forms very strong bonded 3D framework in which the 8a tetrahedral sites and 16c octahedral sites form a 3D interconnected interstitial vacancies. Intercalation of additional lithium ions into the spinel structure $Li(M_2)O_4$ displaces all the lithium ions at 8a and forces them to move to 16c sites.

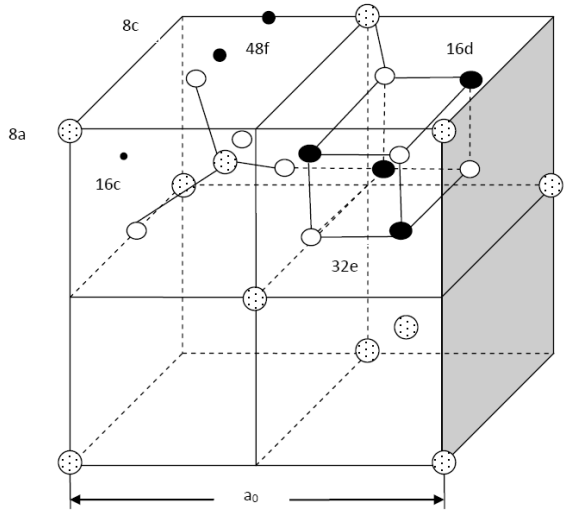


Figure 2.12 Two quadrants of cubic spinel structures

Compared to the layered $LiMO_2$ cathodes discussed above, the spinel framework $Li_xMn_yO_{1-x-y}$ cathodes type has more stable structure, so the voltage would not drop sharply and achieve relatively flat voltage plateau.

C. Olivine framework $LiFePO_4$ cathodes

The olivine structure of $LiFePO_4$ shown in Figure 2.13 has a 3D $FePO_4$ framework that is very stable at high temperature. A small volume change between $LiFePO_4$ and $FePO_4$ provides a flat voltage versus SOC in accordance with the Gibbs rule, which is a very remarkable advantage for this type battery. However, this structure also limits lithium ions to move in 1D channels. The movement of lithium ions could be easily blocked by the other atoms or particles if they are big enough. However, $LiFePO_4$ particles are small and rod-shaped and lithium ions channels are in parallel with this morphology, lithium ions can continually move within the channels in this morphology.

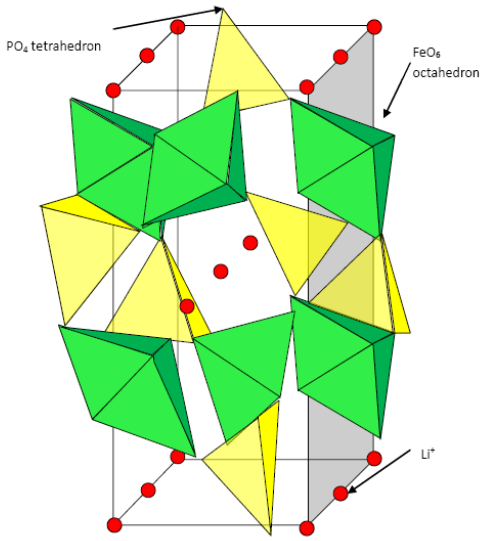


Figure 2.13 Structure of $LiFePO_4$

Generally, depending on the fact that intercalation mechanism is the main one in Li-ion batteries, the crystal structure change influences the characteristics of Li-ion batteries significantly. Comparing the three structures discussed above, $LiFePO_4$ cathode type is the most stable one, which can provide a long voltage plateau, moreover, the stable structure makes $LiFePO_4$ cathode type has superior thermal and chemical stability, which induces that this battery type can handle high temperature and is much safer. The layered $LiMO_2$ cathodes type has a high energy density and a large capacity because lithium ions can conveniently move inside its structure. Spinel framework LixMnyO1-x-y cathodes has high OCV due to Mn^{4+}/Mn^{3+} redox couple, however, the capacity is relatively lower.

2.4.2 Anode materials

In the Li-ion battery market, graphite is used most widely as an anode material. Graphite exists in several forms, from a crystalline state to an amorphous state. These anodes can be classified into 1) soft carbon, which can easily be modified by high temperature 2) hard carbon which cannot graphitize even at high temperature. Soft carbon has a large hysteresis in its potential profile, which induces a loss of stored energy. While the cycleability of soft carbon is poor, the capacity fade would be larger after several cycles. Therefore, hard carbon is popularly used in the battery market [14].

Another attractive alternative anode material is the alloys based on Sn and Si. However, the volume change is very large and the resulting alloys are brittle. So some transition metals are involved to stabilize the structure of the anode [5].

2.4.3 Electrolyte materials

There are two popular electrolyte materials existing at present. One is based on non-aqueous organic solvents, the other on polymer electrolytes [5, 14].

A. Non-aqueous organic solvent based electrolytes

As discussed above, an aqueous electrolyte cannot be used in the Li-ion battery, so inorganic salts dissolved in organic solvents are used as electrolytes. A perfect electrolyte material should have high ionic conductivity, good stability and excellent safety. $LiPF_6$-doped organic solvents are the most common electrolyte in the market today.

B. Polymer electrolytes

There are two types of polymer electrolytes, one is gel electrolyte and the other is dry polymer electrolyte. These polymer electrolytes have low cost and can be easily compacted in the manufacturing process.

Gel electrolytes are consisting of an inactive polymer matrix and a lithium salt solution. These electrolytes flow like liquid at high temperature and behave as a rubber below a glass transition temperature.

Dry polymer electrolytes contain a polymer and a lithium salt. At room temperature, the ionic conductivity of these electrolytes is low. Due to the segmental motions of the polymer chains, the ionic conductivity will increase with temperature.

2.5 Battery management system (BMS) for Li-ion batteries

BMS is the battery pack's brain, which consists of the electronic circuits to provide

- Controlling
- Monitoring
- Error
- Calculating
- Cell balancing

on the operational parameters during charging and discharging of the Li-ion battery such as currents, voltages, and the internal and ambient temperature. The monitoring should protect the circuits by disconnect the battery from the loads or generate alarms when parameters grow out of limit [15, 16].

High current flow through the battery cells or pack can lead to high internal temperatures [17]. To avoid high current flow it is good to know how much maximal current could be drawn to charge or discharge the battery for various SOC level. The BMS should be able to prevent high current flow through the battery if it happens.

The main objective of all BMS is to protect the battery pack or cells from harm, increase the life time of the battery and to maintain the battery voltage in the required region. To achieve these objectives some of the following functions need to be implemented [15].

2.5.1 Definition of significant parameters in the BMS

The most important parameters to monitor in the Li-ion battery are the current, voltage, temperature and to use these to calculate the SOC. SOC of the battery is the level or amount of energy which could be produced or left in the battery pack.

$$SOC = SOC_{OCV} + \Delta SOC = SOC_{OCV} + \frac{\int_0^t Idt}{Q_{tot}} \quad (2\text{-}20)$$

There are several methods to estimate SOC, some depend on the battery chemistry but most depend on the measure of some parameter which is varied with the SOC e.g. by knowing the current flow through the battery then ΔSOC could be calculated. It's a rate of how much of the battery capacity C is used or how much it is charged in a percentage ratio and then from the fingerprint of the battery, which is the presented in figure 5-10, the OCV will be found which is the actual voltage level of the battery pack (when the battery is disconnected from the circuit, the voltage over it corresponds to OCV). This will yield the corresponding SOC_{OCV} and by adding this to ΔSOC the actual SOC is obtained [18]. A more detailed explanation will be provided further on in Appendix A.

2.5.2 Task of the BMS

A. Monitoring

The role of monitoring is to check the levels of the battery pack, monitor cell characteristics or to manage the system. Monitoring will only indicate that the levels have not exceeded the limitation values. To prevent false alarms or noise signals, the monitoring has a time delay before notifying that the level has been exceeded. The levels of interest are parameters such as pressure, temperature, voltage and current [16].

B. Measuring

Measurements in BMS are usually including for each cells voltage and temperature, and current is typically measures for the battery pack. It will supply the size information in addition to what is visible from monitoring [16].

C. Calculating

Calculating is the action of using measurement data of accurate battery cell characteristics to calculate the desired parameters [16].

D. Error

In order to provide data or information from monitoring, measuring and calculating to another unit or subsystem, communication is needed. It can be as simple as just using some flashing lamp or light emitting diode (LED) to convey that the level of some parameter has been exceeded. Depending on the inclusion of more refined protocols such as data set and bus structure, the communicating can be more advanced [16].

E. Control

Control means that the BMS has control over the battery cells and pack, such as connecting and disconnecting the battery during charging and discharging periods, when the current, voltage and temperature exceed the minimum or maximum limitation level of the battery pack or cells [16].

D. Cell balancing

The balancing system is not a necessary function for all battery types, depending on the chemistry of the cell. Due to small differences of internal impedances or other factors of the cell, unbalances may occur [16]. Different ageing characteristics in series connected cells as well as different temperatures can cause unbalance at the battery pack. During charging of a battery pack which consists of multiple chain connected cells, if one of the cells is charged before the other, it leads to damages to the cell due to building high temperature and pressure. This is due to the fully charged cell becoming overcharged while the other cells will continue their charging. For every charge and discharge period the weak cell will become weaker and it damages the battery pack. During discharge, the weakest cell will be discharged much quicker than other cells. This will lead to excessive discharge, ageing and damage of the cell [15].

2.5.3 Design of the BMS

The model of the battery control system will be used to monitor one of the system solutions in section 4, and by testing and investigation improve the controller. The controller should be adapted to the behavior and working area of the Li-ion battery as presented in Figure 5.11. The controller will take care of taking the Li-ion battery to the target level after every discharge. When the alternator is on it will charge the battery pack back to the original level of the battery SOC, since charging and discharging the Li-ion battery in some intervals many times affect the aging but not as much as compared to other battery type. Figure 2.14 shows the steps of the charge and discharge controller system.

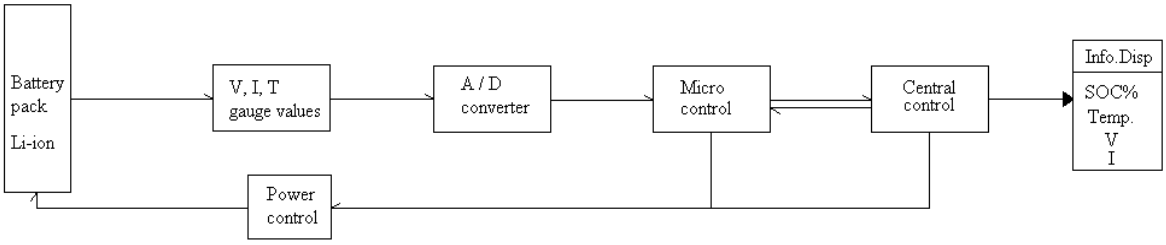


Figure 2.14 Scheme of the controller system for Li-ion battery packs

The information is provided to the micro controller through an A/D converter. It is then communicated to the central controller to calculate and combine the values with the algorithm to make sure all voltages, currents and temperatures are within the limitation values during charging and discharging cycles. If the cell's or battery pack's characteristic levels exceed or fall below the limitation region, the central and micro controller should send an order to the power controller (a relay could be used as power control) to cut-off the Li-ion battery pack from the circuit directly [17, 19], to avoid damaging the Li-ion battery pack and to increase the safety and quality of the battery pack.

When cut-off occurs for some reasons stated above, the engine should start directly again and the alternator supply the energy to the system.

2.6 The final scope of the thesis

Comparing the conclusion drawn in this chapter with the scope explained before, the final scope of this thesis work is to parallel connect a lead-acid battery with a lithium ion battery in vehicle applications, which can be seen in Figure 2.15.

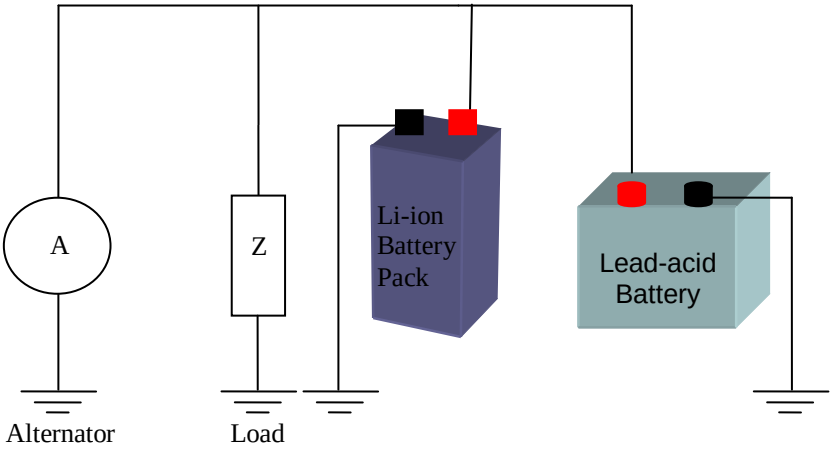


Figure 2.15 The final scope of the work

The lead-acid battery will be the main power supply in this system. When the driver starts the vehicle at first, the lead-acid battery will provide high power to activate the engine, after that, the alternator can charge both batteries if they need to be charged. During start-stop application, the engine will be off in order to decrease the fuel consumption and CO_2 emission. The electronic equipment (the loads) will be supplied with the current only from the lithium ion battery. When the engine starts again, the alternator should recharge the lithium ion battery. The batteries should not be used to charge each other.

3. Charge algorithms

3.1 Charge methods for the Li-ion battery

Charging and discharging Li-ion batteries demand observing some precautions if the CC-CV method is used, this is more important when multiple cells are involved. In this section different types of Li-ion battery charging methods will be presented. The charging of Li-ion batteries is more complicated compared to that of other batteries like NiMH and Ni-Cd batteries. The normal method which is used for charging Li-ion cell is the Constant Current – Constant Voltage (CC-CV) method. This charging strategy is of low cost compared with other charging methods, because less electronic components are involved. The figure below shows how the CC-CV method works [20].

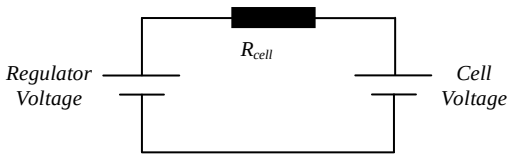


Figure 3.1 Equivalent circuit model for the CC-CV method of charging a Li-ion cell

Implementing this method, the Li-ion cell could be connected to the output terminal of a voltage regulator with a current limit. Applying physical laws to the circuit in Figure 3.1 the charging current can be calculated as follows:

$$I_{charge} = \frac{V_{regulator} - V_{cell}}{R_{cell}} \quad (3\text{-}1)$$

If I_{charge} is larger than the current-limit of the regulator I_{limit}, it means the cell will be charged by a constant current. As the cell is charged, the voltage increases while the charging current decreases. Near full-charge I_{charge} becomes very small. In this time the cell is charged and can be disconnected from the voltage regulator. This method does not work so well when applied to multiple cells, because the charging method needs some kind of balancing between those cells, e.g. the battery pack consists of three cells with max voltage of 4.2V each, the voltage regulator is set to three times this voltage, which is 12.6V. In the process of charging, if one cell reaches 4.2V before the other two, and suppose the voltage in these are 4.1V, the open circuit voltage of the battery pack will be 12.4V. Since this value is less than the regulator voltage, it will continue to charge the battery and the cell which is already fully charged becomes overcharged and damaged [20].

The next charging method is called parallel or taper charging method. The cells are in series in the battery, and are charged with a constant current. When the battery is charged, the current flow will start to decrease and the charging will stop, when the current reaches one-tenth of the initial current. The benefits of this method is its simple circuit, full charging of all cells in the battery and switching once one cell reaches full charge [20].

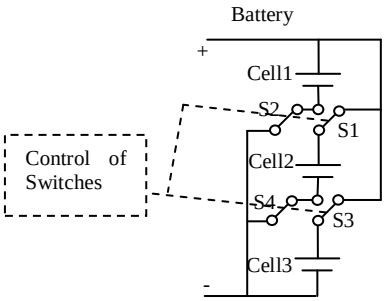


Figure 3.2 Parallel charging method

In the Resistive Equalization Method the battery cells are connected in series and charged with a constant current (Figure 3.3). The concept of this method is that when one cell is charged before others cells, as in the description above, it will discharge a bit with their equivalent parallel resistor. This process will repeat until all cells are charged [20].

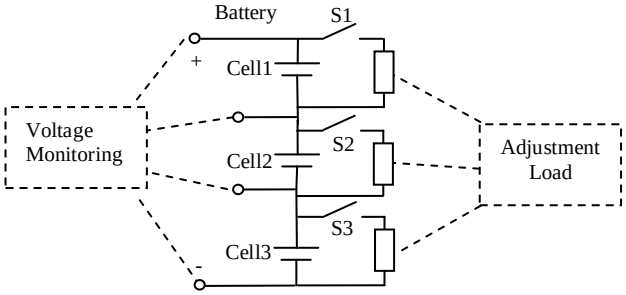


Figure 3.3 Resistive equalization method

Transformer equalization method is similar to the resistive equalization method but uses a transformer instead of the resistive component to balance the cells (Figure 3.4). It transfers the amount of excessive charge of the fully-charged cell to the other cells and balances their voltage [20].

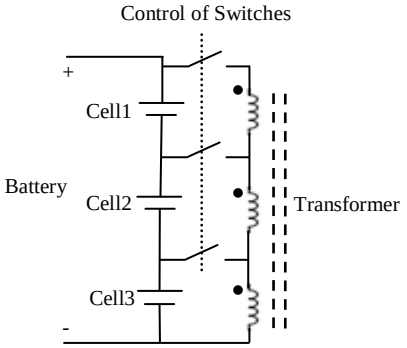


Figure 3.4 Transformer equalization method

The switched capacitor equalization method works as the previous methods; the cells are in series, however every cell has a parallel connected adjustable capacitor for balancing the voltage over the cells. The benefit of this method is that there are no

resistive losses and there are no inductance, transformer and resulting disturbances. However, each cell requires a single-pole double-throw switch as well as capacitor [20].

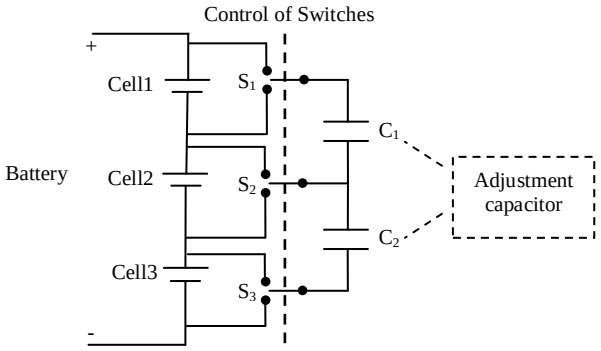


Figure 3.5 Switched capacitor equalization method

3.2 Charge methods used in the lab

The charging method which will be used for this thesis is CC-CV, with the motivation that less electronic are included and therefore both cheap and less time-consuming for testing.

The general charging characteristic of the CC-CV method can be seen in Figure 3.6. According to the Li-ion battery's basic information, the maximum voltage is 16.6V, and hence this is the upper limit. The charge voltage rises rapidly to the cell's upper voltage limit and is subsequently maintained at that level. As the charge approaches completion the current decreases to a trickle charge. Cut-off occurs when a predetermined minimum current point, which indicates a full charge, has been reached.

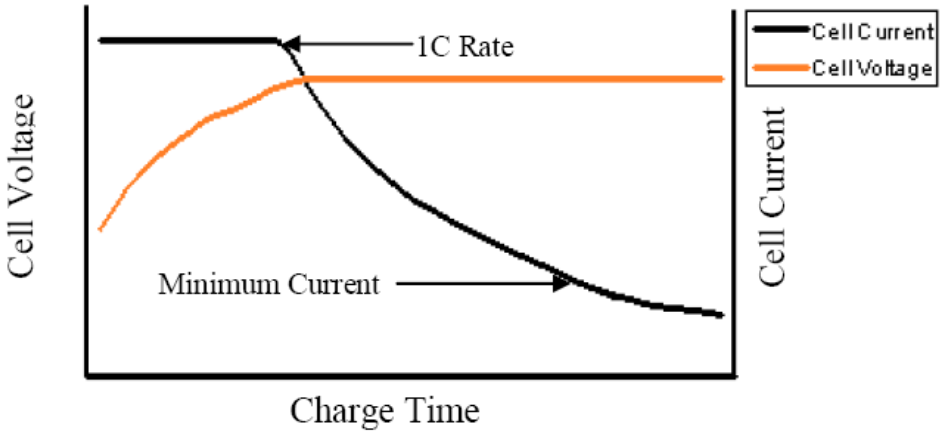


Figure 3.6 The Li-ion charging characteristics

4 Tests

In section 4.1 and 4.2 the experimental tests performed at the lab bench are explained to get more familiar with the system, prior to be implemented in the vehicle.

4.1 Test setup for lithium ion battery

Figure 4.1 shows the battery pack with two cells in parallel and four cell pairs in series. The charging system looks like the following:

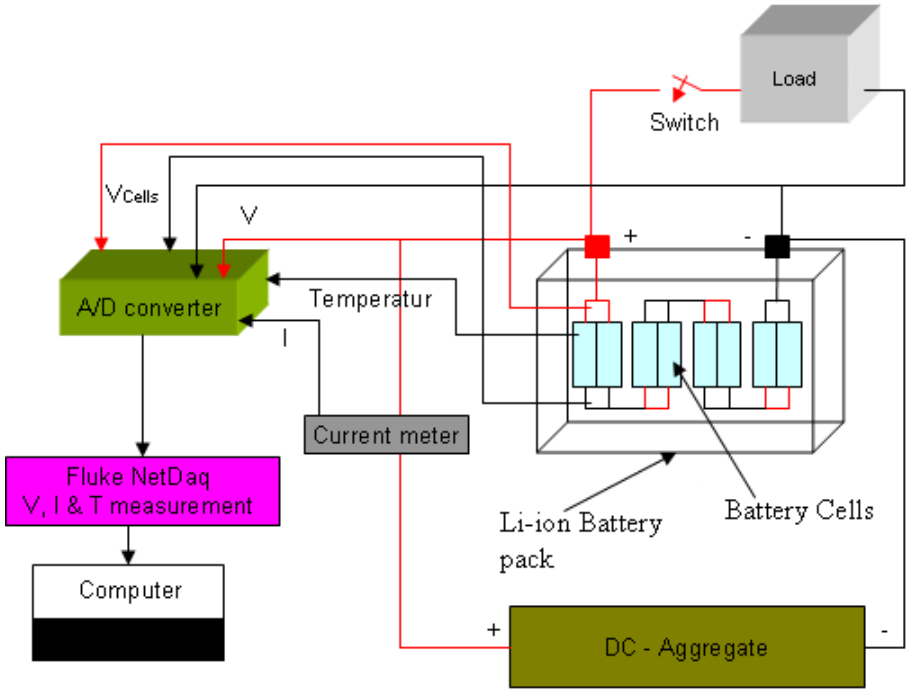


Figure 4.1 Sketching charge/discharge system.

Figure 4.1 shows the charge and discharge system connection for the Li-ion battery pack. The charging method which is used in this case is called constant voltage. The constant voltage method is basically a DC power supply which in its simple form consists of an AC/DC converter and transformer to step down the voltage to the required value [15]. The Fluke 80i -110s is the current meter to measure the current flow and is connected to the A/D converter in turn to send the digital data signal to the Fluke NetDaq for saving and collecting the measurements in the computer. The voltage over the battery pack and cells are measured connecting two cables in parallel on the plus and minus pole of each cell and for the total battery pack the same procedure is used as for the current measurements. For temperature measuring, k-type thermocouple is used, one end is pasted on the surface of the battery cell and the other one is connected to the A/D converter. The signal is sent to the Fluke NetDaq and subsequently to the software program called NETDAQ used at the computer. The voltage and temperature is monitored manually as well by using Fluke 77 Multimeter and Fluke 52 Thermometer, to be sure that the voltage and internal temperature ($T < 45$ degrees) are in the safety intervals, in order to avoid overcharging the battery.

To discharge the battery pack, a variable load is used, which can control the output current from the battery pack. The maximum charge and discharge current for the battery; during the lab 50A is assumed for user-safety reason.

4.1.1 Charge and discharge tests

The following steps explain the stages of the battery tests.

1. When the battery pack reaches its fully charged level, the voltmeter is used to measure every battery respectively and yield every battery's voltage. This step will be done every time when charging or discharging the battery system in order to monitor self-balancing, which will beneficial in avoiding damage to the system.

2. Below is a table of different constant charging currents used to let the batteries reach a fully charged state. During this process different voltages and times are measured, yielding:

- voltage versus time plot
- voltage versus SOC plot
- power versus time plot
- current versus SOC plot
- temperature versus SOC plot

SOC can be calculated according to

$$SOC = 1 - \int_0^t \frac{Idt}{Q_{tot}} \quad (4\text{-}1)$$

Qtot is the total capacity of the battery pack and I is the current flow in or out of the battery pack.

Table 4.1 Different charge rates and constant input voltage during charge

Icharge	C-rate	Vinput
10 A	1/3 C	16.6 V
20 A	2/3 C	16.6 V
30 A	1 C	16.6 V
40 A	4/3 C	16.6 V
50 A	5/3 C	16.6 V

3. From the supplier, it is known that the cut-off voltage is nearly 12.12V. The battery pack can be discharged with different constant currents the specific data can be seen in Table 4-2. During this process, different voltages as well as time are measured and draw

- voltage versus time plot
- voltage versus SOC plot
- power versus time plot
- current versus SOC plot

- temperature versus SOC plot

Table 4.2 Different discharge rates and the full-discharged voltage

Idischarge	C-rate	Vcut-off
10 A	1/3 C	12.12 V
20 A	2/3 C	12.12 V
30 A	1 C	12.12 V
40 A	4/3 C	12.12 V
50 A	5/3 C	12.12 V

4.1.2 Open circuit voltage test

One of the most importing characteristic of the battery is to define the OCV versus SOC, by knowing this; it will be easy to handle the battery.

To measure the open circuit voltage, the fully charged lithium ion battery pack is discharged by 1Ah until it reaches cut-off voltage. The discharging can be done in several intervals of 5% decreases of SOC from 100%. The following equation is used to calculate the time of discharge.

$$Time_{discharche} = \frac{Q_tot}{I_{discharge}} = \frac{30Ah}{1A} = 30h \quad (4\text{-}2)$$

The discharging time of each stop gives 1.5h discharging time, so every 1.5h the test procedure should stop in order that the voltage recovers to the steady state value and then continues to discharge again.

4.2 Proposals of system solutions

This section concerns the investigation, testing and explanation of different methods of using the Li-ion battery in a vehicle with Stop/Start function.

4.2.1 System solution A

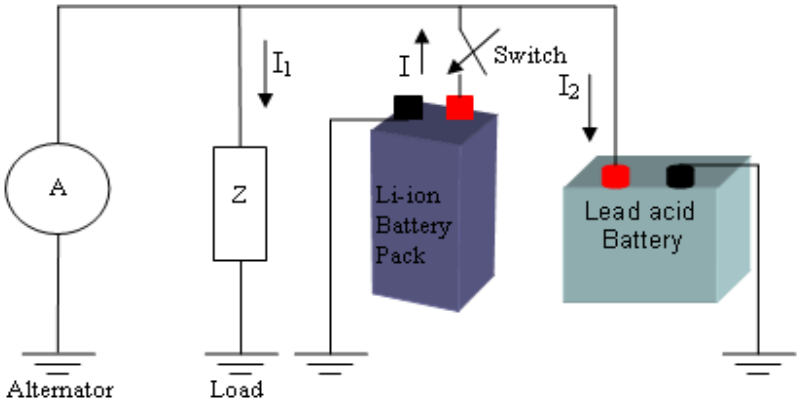


Figure 4.2 The original battery system solution in the vehicle when the alternator is off

The case in Figure 4.2 shows that to achieve the goal of the thesis, it is needed to use the battery which has been investigated, mainly due to its higher voltage level and energy output.

The switch is used, as shown in Figure 4.2, to protect the Li-ion battery pack from any accidents, such as over-discharge/charge, and high temperature which all can cause problems to the battery. The benefit of this model is that it is cheap since it does not require any electronic components added to the system and is thus simple. The disadvantages are the fact that during charging, the voltage supply from the alternator is too high for the lead-acid battery, because it's already fully charged at 12.9V. Thus if it will be overcharged for shorter periods it is acceptable, but if this system solution will be used in vehicles it will cause damage to the lead-acid battery. However, not only the lead-acid battery will be affected. The Li-ion battery will, during stop time or when the alternator is off, start to charge the lead-acid battery while at the same time supplying the loads, since it has higher voltage potential. Therefore, the model is prone to cause quicker aging and damage to the batteries.

To improve this system solution, some modifications to the usage will be needed. Figure 4.3 shows the behavior of the Li-ion and lead-acid batteries.

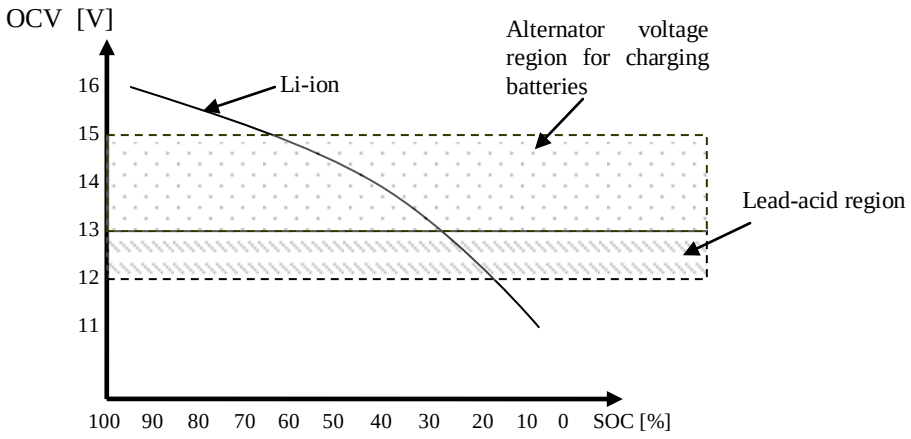


Figure 4.3 A comparison of OCV of Li-ion battery and lead-acid battery

The OCV versus SOC for Li-ion and Lead-acid batteries are compared in general above. When the working region is between 70%-55% SOC, the Li-ion battery pack will charge the lead-acid battery as well as support the loads, since the voltage of the Li-ion batteries is higher in that area than that of the lead-acid batteries. One solution is, although complicated, that if the internal resistance of the lead-acid battery is increased, less current will flow through it and it does not matter if the voltage is high. Therefore, it could be assumed that the Li-ion battery only supplies the loads during stop time. Another method would be to move the working region from 15.2V to 13V of the Li-ion battery. However, it does not give any benefits because it is a region that causes a decrease in the life time of the battery pack. As shown in Figure 5.10, it is not good to process the Li-ion battery in that region due to the slope being very steep down. It leads to fast discharge and decrease in the life time. Other different system solutions to deal with this problem will be presented below.

4.2.2 System solution B

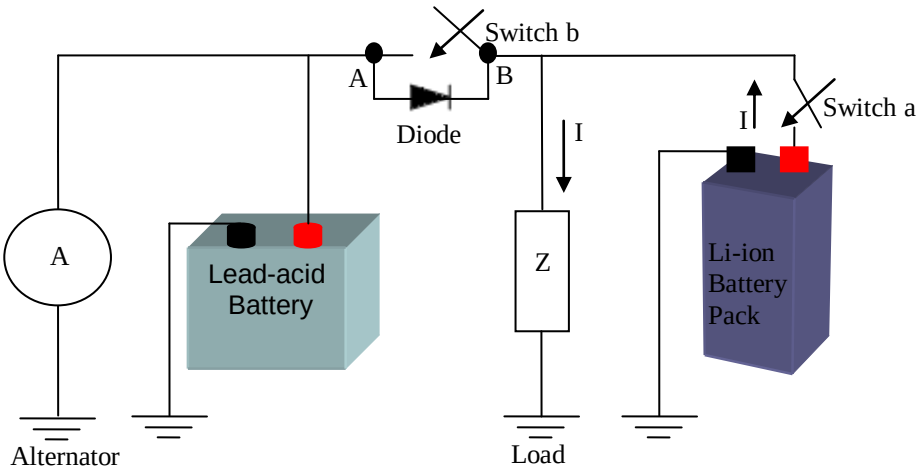


Figure 4.4 Improved battery system solution A in vehicle when the alternator is off

In this case the alternator could be assumed to supply a maximum of 15.2V during charging. As seen in Figure 4.4, a Schottky diode which has low forward voltage drop and better system efficiency [22], can be connected in parallel to switch b to avoid any charging of the lead-acid battery during stop time, as mentioned before. Some important aspects in car manufacture are to deliver a safe and high quality vehicle to their customers. To maintain this relay or switch should be connected in parallel to the diode so that in the case of malfunction there exists a back-up feeding for the electronic equipment. By using the switch and sending a warning signal to the central electronics system, a lamp should notify the driver about the problem in the system. The diode is forward biased with a 0.15-0.45 V drop, so the current can only flow in one direction, from A to B in this case. The advantage is that the system can work better than the previous one, since the issue of charging the lead-acid battery with Li-ion battery during stop time is avoided. A disadvantage can be that more electronic components are needed and thus the cost will increase.

4.2.3 System solution C

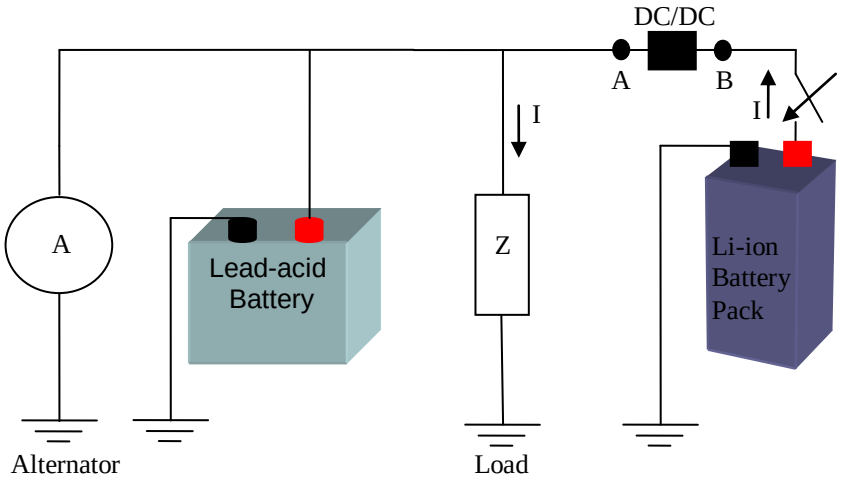


Figure 4.5 Improved battery system solution A in vehicle when the alternator is off

For the improvement of the system solution above, a buck/boost DC/DC converter could be used, which lower the voltage at node A during discharge to the same voltage potential as the lead-acid battery to avoid charging it and to transfer up to 16.6V at node B during charging period. It can also decrease the maximum voltage to 16.4V margin which can lead to easier control voltage over the battery pack or cells. The benefits of this model are that more power can be taken from the Li-ion battery pack because of increasing SOC region and the fact that this model can be used in-vehicle. The disadvantages are the high cost of a 1kW DC/DC converter and power losses in the DC/DC converter, but with respect to getting high energy amount, the power losses could be ignored compared to the power that is taken from the battery.

4.3 Test performed in vehicles

The Li-ion battery pack parallel connected with the lead-acid can be presented as follows:

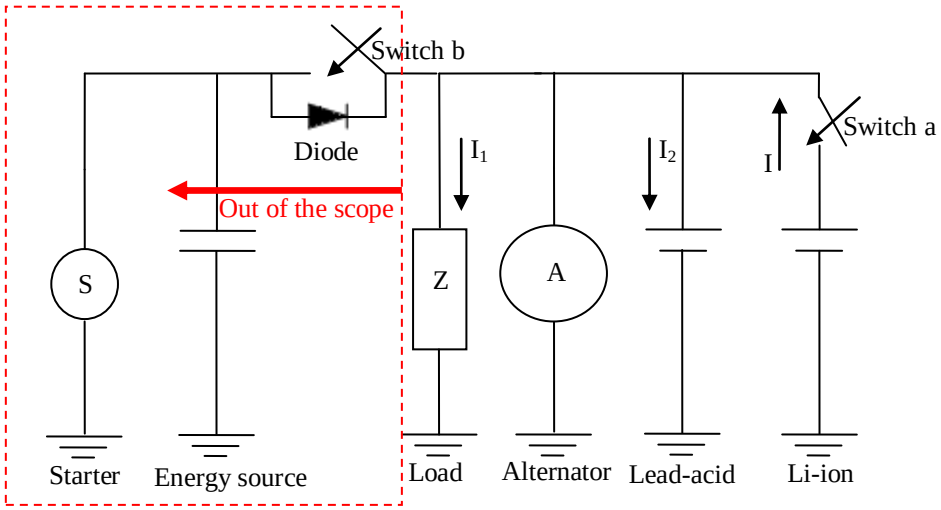


Figure 4.6 Connection system of both battery types in the vehicle

Figure 4.6 represents the first system solution A in the vehicle, which is able to work with Li-ion and lead-acid batteries connected in parallel. The system solution is chosen because there are less electronics used which means low cost and with the benefit that this system solution already has been explained on the lab bench in section 5 and performed well. As seen from Figure 4.6, the "out of the scope" region is not included in the result part, which means when the engine starts again after each stop, instead of the lead-acid battery another energy source will support the starting system. Thus, the interesting part is to investigate how the Li-ion battery will supply the loads during stop time. In this case the alternator of the vehicle will supply 15.2V which is the maximum output voltage it can supply.

4.3.1 Electrical management system in the vehicle

The brain of the electronics part in vehicle is called CEM (Central Electronic Module); it collects all data and measurements of different electronics part and all warning signals that may arise. All communication with other different modules occurs via CAN (Controller Area Network) or LIN (Local Interconnected Network) buses. The lead-acid battery monitoring in the vehicle is communicated through LIN bus which is connected to a battery sensor for measuring the current, voltage, temperature and then calculate SOC of the lead-acid battery by those parameters. The same method will be used to measure the equivalent parameters for the Li-ion battery pack. However only current and voltage values will be possible to be measured since the SOC for Li-ion battery is different from the Lead-acid battery due to different characteristics. From the measured current and voltage the SOC can be calculated to determine the relay switching in the Simulink model.

4.3.2 Simulink model for calculating SOC and switching relay

The calculation of SOC for the Li-ion battery pack will be done in the MATLAB software by using Simulink. Real-time workshop is another software wrap for

MATLAB. It used in Simulink to generate C-code to the MABX (MicroAutoBox), from the Simulink model to process the SOC calculation and control switch A in the vehicle. Figure 4.7 explains the calculation of SOC and the procedure of switching switch A. The complete Simulink model is presented in appendix A for more understanding of the system.

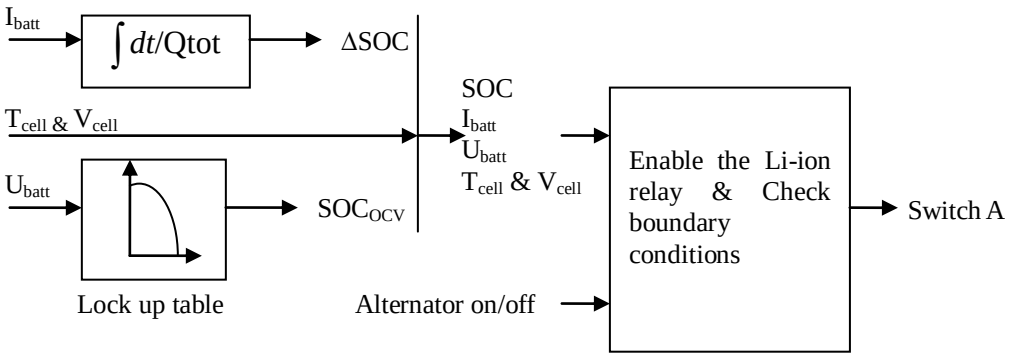


Figure 4.7 Charge and discharge battery model chart of Li-ion battery pack

Figure 4.7 shows that the battery current and voltage is measured with the battery sensor; by integrating the current flow and dividing with Q_{tot} yields the ΔSOC, which is a measure of how much of the Li-ion battery SOC is used or charged. By triggering the correct value of the battery open circuit voltage, a value of SOC is obtained which is dependent on OCV. The values in the look-up table obtained from lab results section 5 are acceptable. By adding ΔSOC and SOC_{OCV}, the correct SOC of the Li-ion battery pack is yielded. Thus, the SOC estimation is based on the open circuit voltage and current [18].

To control the system, the MABX and the measurements system described in section 4.1 will be used, which imports the signals from the battery sensor, such as the total voltage over the battery pack, current. For each cells the temperature and voltage will be monitored separately. Information such as whether the alternator is on/off will be taken from the main control system of the vehicle. The Simulink model will be uploaded to the MABX and the measurements, controlling and switching will occur accordingly.

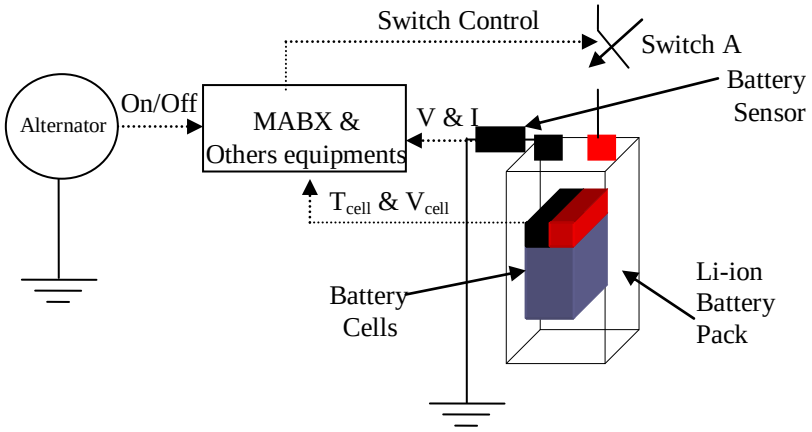


Figure 4.8 The controller system for the Li-ion battery pack

By other equipments, it is referred to those instruments which have been used in the lab bench in section 4.2.

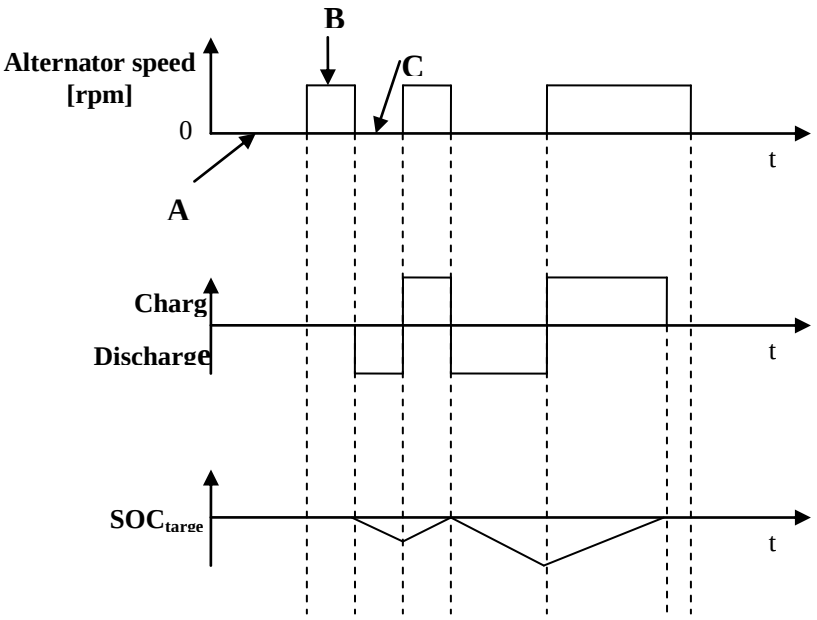


Figure 4.9 The function of the engine to be on or off affects the charge and discharge of the Li-ion battery pack

Based on all those parameters and steps the control system will be designed; firstly the signal determines the positions of switch A. When the vehicle is off or parked at region A the relay is off and no SOC measurement occur; when the vehicle starts it gives one trigger, and since switch A is off it leads to measuring the correct OCV and thus the actual SOC_{OCV} value will be presented. Region B constitutes the engine being on again and all energy will be supplied by the alternator to the loads and charging the batteries- Relay A can be switched on until the battery is charged; region C is during stop time or the time where the Li-ion battery pack is processing.

5. Results and discussion

5.1 Lithium ion battery

Figures 5-1 and 5-2 show the characteristics of the Li-ion battery pack during the tests at room temperature 25 ℃. The measurement time is assumed to 1 sec and the equations which have been used are presented below. The following formula is used for calculating the capacity of the battery pack in which I and t is the charge/discharge current and time period respectively,

$$C = \frac{\int_0^t Idt}{60sec \times 60min} \quad (5\text{-}1)$$

To calculate power,

$$P = UI \quad (5\text{-}2)$$

Where U and I are charge/discharge voltage and current. The energy can be estimated as follows:

$$W_{out} = \int_0^t Pdt \quad (5\text{-}3)$$

$$W_{losses} = \int_0^t RI^2 dt \quad (5\text{-}4)$$

where R_{int}=0,01Ω (R_{int}=2*R, R=0.005 Ω) is the internal resistance of the battery pack at room-temperature by modification. The total available energy is

$$W_{available} = W_{out} + W_{losses} \quad (5\text{-}5)$$

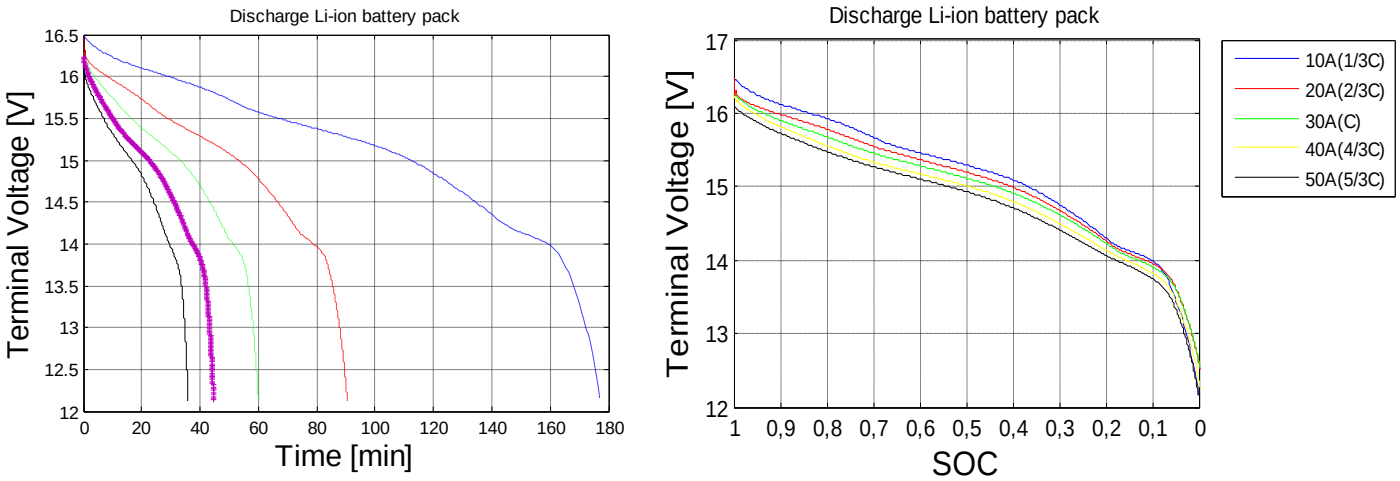


Figure 5.1 Measured Terminal Voltage vs Time (left) and Terminal Voltage vs SOC (right) at different discharging currents

As seen from Figure 5.1, from the right hand side, the internal resistance can be calculated by choosing two different points between the highest and lowest curves and then it will give that

$$R_{int} = \frac{\Delta V}{\Delta I} = \frac{0.4V}{40A} = 10m\Omega \quad (5\text{-}6)$$

The value corresponds well with the manufacturer's value of internal resistance.

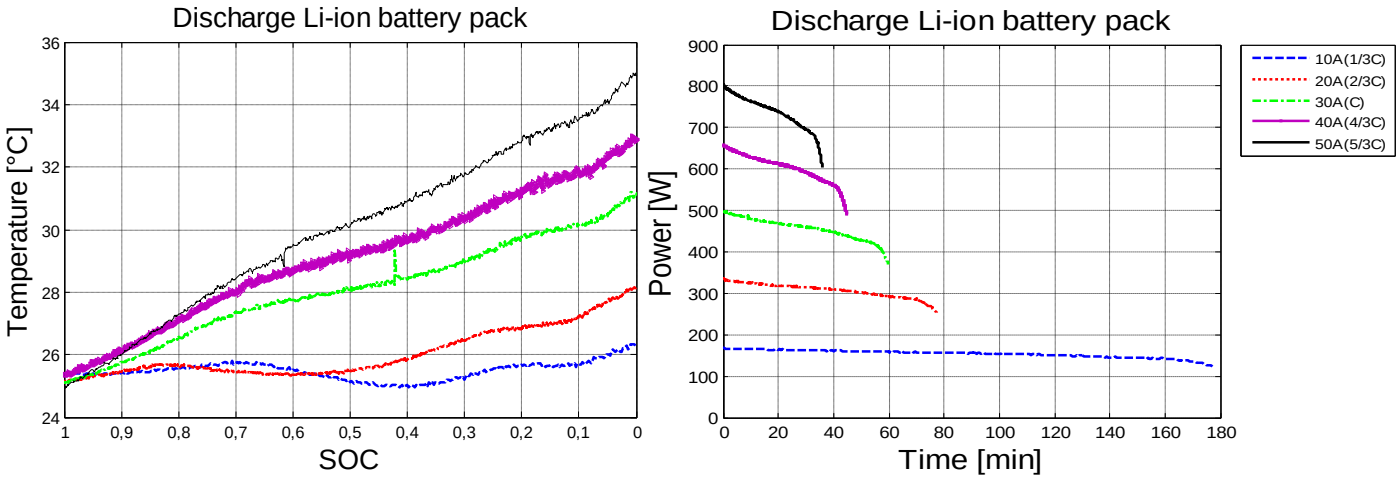


Figure 5.2 Measured Temperature vs SOC (left) and Power vs Time (right) at different discharges current

Table 5.1 Energy consumption during dicharge

Energy [J]	W_{OUT} [J]	W_{Loss} [J]	Total Energy [J]
$W_{available\ 10A}$	1633100	10972	1644073
$W_{available\ 20A}$	1644585	22120	1666706
$W_{available\ 30A}$	1637979	33401	1671381
$W_{available\ 40A}$	1615346	44133	1659480
$W_{available\ 50A}$	1589057	53562	1642620

Table 5.1 shows the energy consumption at different discharge rates. The energy loss is highest when discharge rate is 50A, and is proportional to the current squared. As can be seen in the left graph in figure 5.2, even in the highest loss situation, that is, the discharge rate of 50A, the delta temperature is not more than ten degrees, which is much lower than the maximum temperature limitation of lithium ion battery from the supplier. Therefore, the temperature effect of lithium ion battery can be accepted when it is used at room temperature.

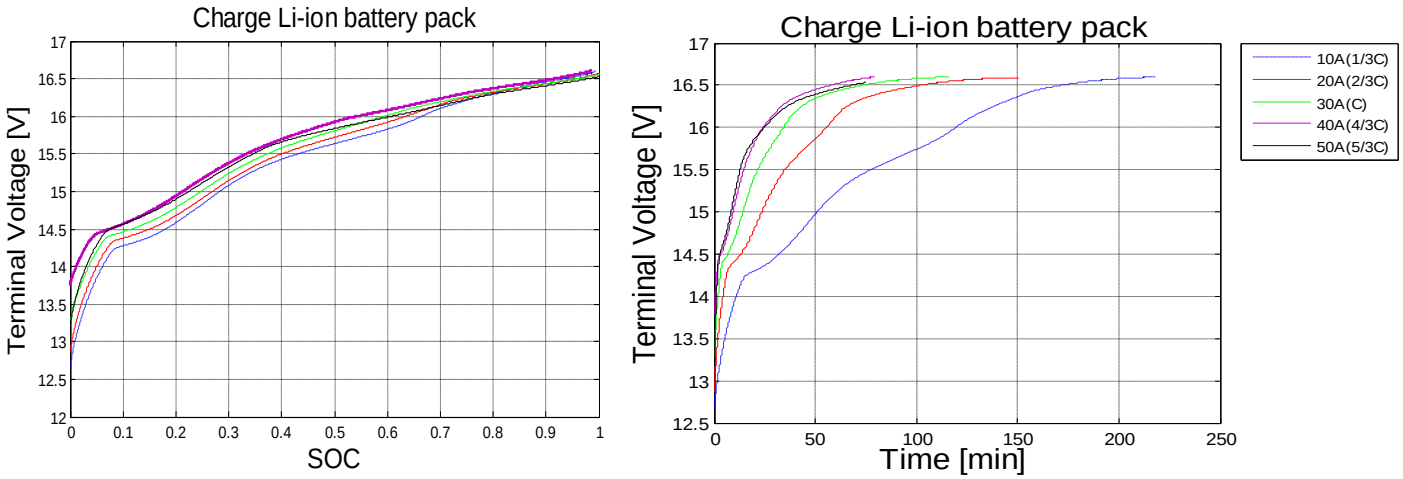


Figure 5.3 Measured Terminal Voltage vs SOC (left) and Terminal Voltage vs Time (right) at different charges current

The charge process can be seen in Figure 5.3. The charge curve is nearly the same as the discharge curve shown in Figure 5.1 and the voltage at each SOC point is also similar as that in Figure 5.2. From this, it can be verified that the reaction in lithium ion battery is reversible.

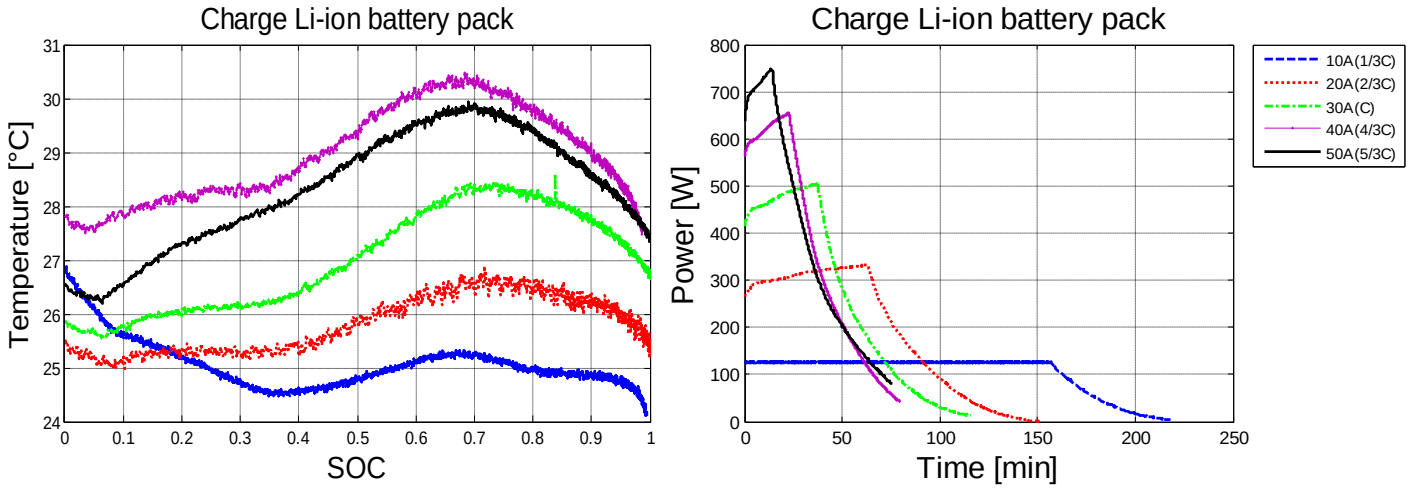


Figure 5.4 Measured Temperature vs SOC (left) and Power vs Time (right) at different charges currents

As seen in the curves in Figure 5.4, the temperature change is smaller than that in the discharge process (Figure 5.1). This point can also be noticed in Table 5.2; the energy loss is less than that shown in the discharge process (Table 5.2).

In this case, the energy loss is mostly spent to increase the temperature of the battery. Therefore, if a cooling system is added into the system, the energy consumed during the charge process would be lower than that in the discharge process.

Table 5.2 Energy consumption during charge

Energy [J]	W_{OUT} [J]	W_{Losses} [J]	Total Energy [J]
$W_{available\ 10A}$	1648584	6057	1654642
$W_{available\ 20A}$	1688275	19372	1707647
$W_{available\ 30A}$	1749889	28609	1778499
$W_{available\ 40A}$	1671247	34112	1705360
$W_{available\ 50A}$	1692547	36290	1728838

Figure 5.5 depicts the charge method of the lithium ion battery used in the experiment, which is exactly the same as that which has been described in Figure 3.6. So the charge method matches the profile discussed before well.

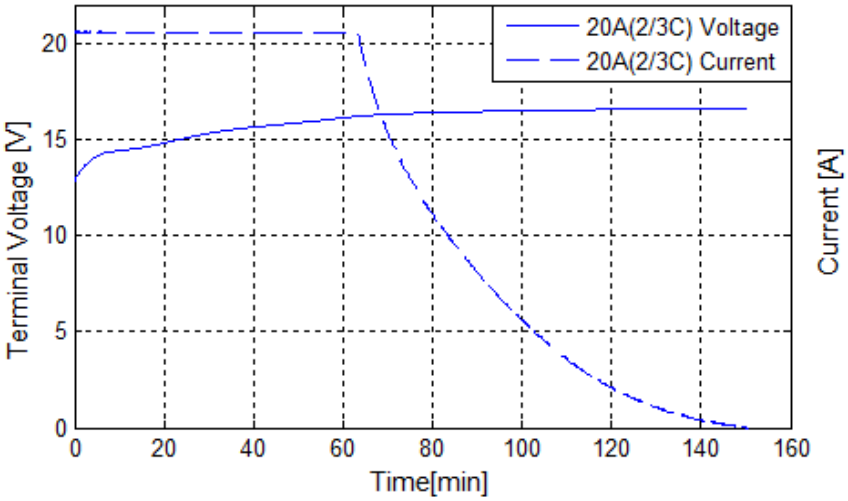


Figure 5.5 Charging characteristics for lithium ion battery in the experiments

In Figure 5.6 and Figure 5.7, there is nearly no difference between each cell, not only in the charge process, but also in the discharge process. However, Figure 5.8 which has been zoomed shows the voltage differences between each cell, although it is not considerably large. Because the batteries are brand new in the work, the difference is not so obvious; however, with the usage period increasing, the aging mechanisms inside the battery and the working situation outside will affect the characteristics in each cell and widen the voltage difference between each cell. This is unavoidable with current battery technology. Therefore, cell balancing is needed to reduce the hazards and improve long-term effects.

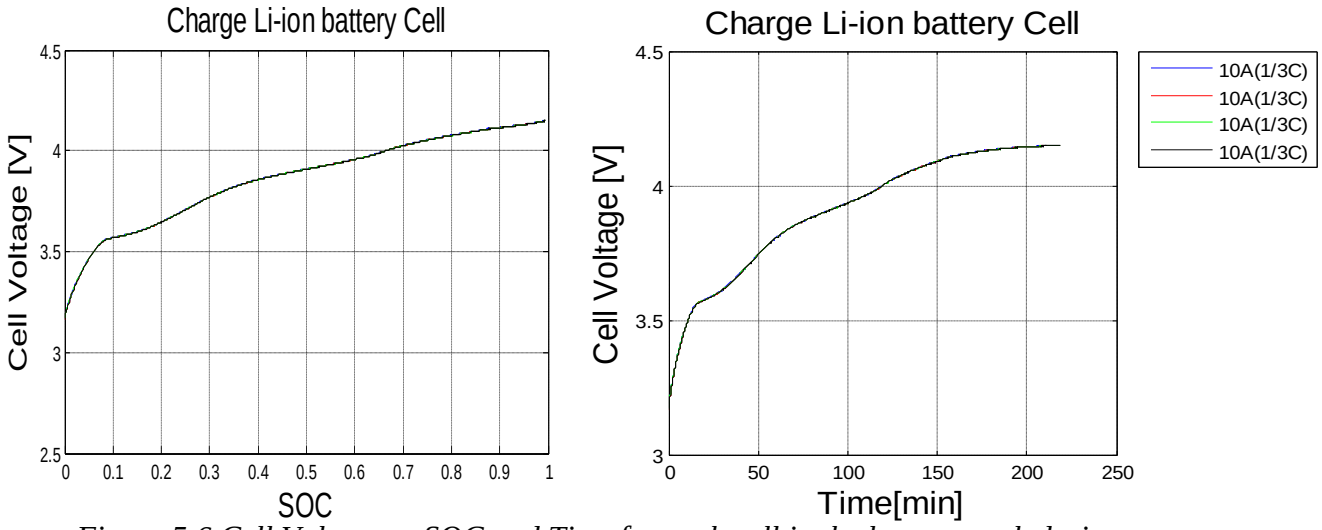


Figure 5.6 Cell Voltage vs SOC and Time for each cell in the battery pack during charging time

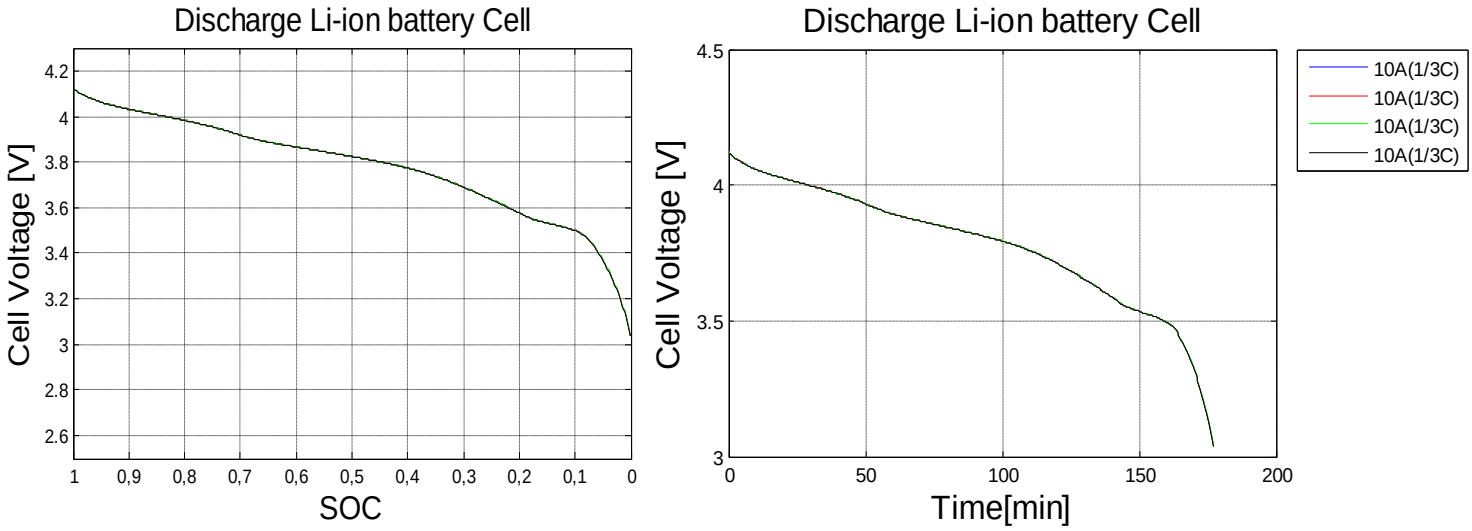


Figure 5.7 Cell Voltage vs Time for each cell in the battery pack during discharging time

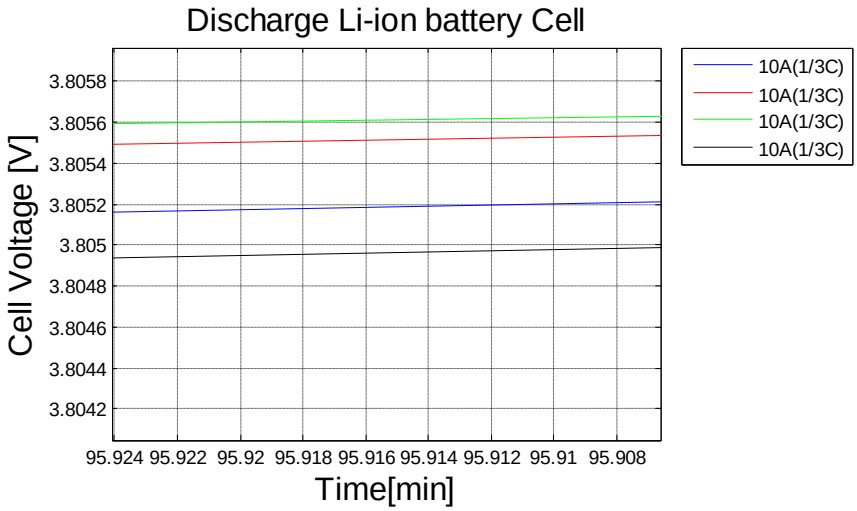


Figure 5.8 Enlarged graphs of Figure 5.7

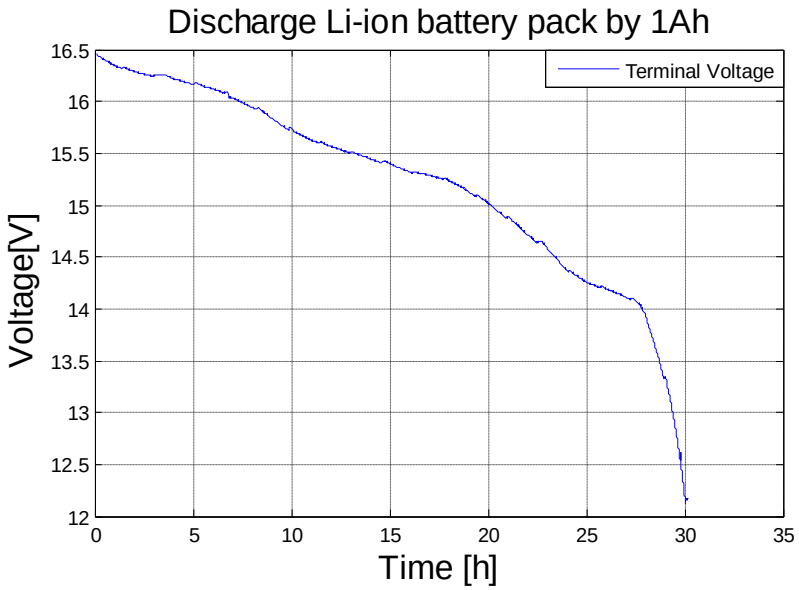


Figure 5.9 Terminal Voltage vs Time by discharging at 1/30C rate

As can be seen in Figure 5.9, the voltage jump appears at every rest phase; the OCV can be measured after the jump when the voltage goes up to steady state and by collecting those points and plotting against SOC. The OCV versus SOC is presented in Figure 5.10 below.

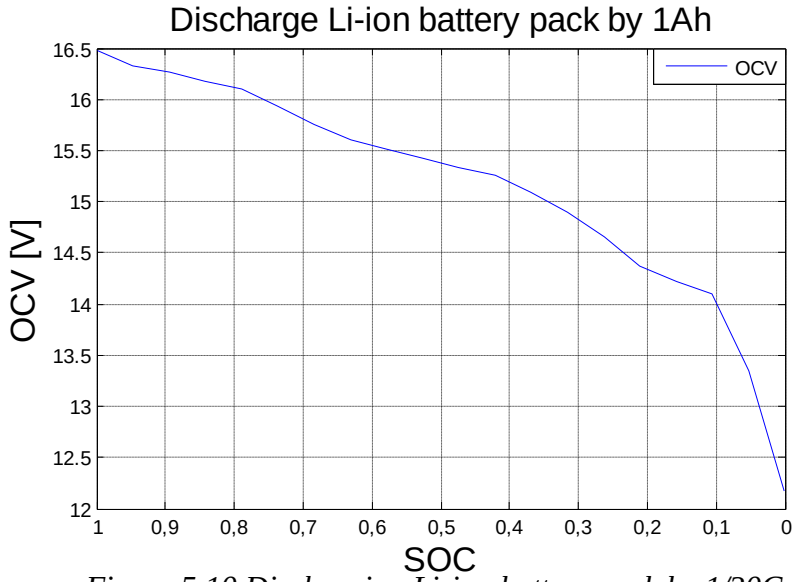


Figure 5.10 Discharging Li-ion battery pack by 1/30C, OCV vs SOC.

Figure 5.10 shows the important graphs which can be called the battery's "fingerprint" because in the next step, by knowing the OCV versus SOC of the Li-ion battery, the charge/discharge controller model and boundary conditions will be adapted to develop the battery management system.

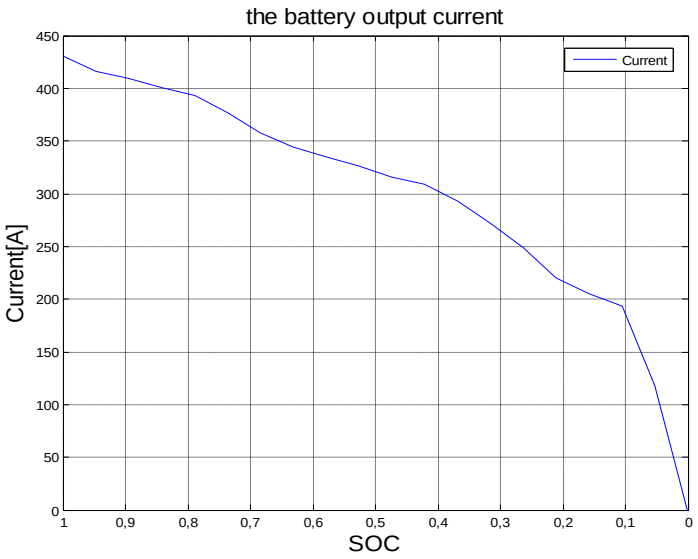


Figure 5.11 The current available for utilization versus SOC for the Li-ion battery pack

An interesting fact is the amount of current possible to obtain/take from the Li-ion battery pack for each SOC level. This might be one of the reasons why replacing the Li-ion battery for the lead-acid battery in the vehicle is not perfect or even possible. That maximum current is calculated as:

$$I_{max} = \frac{OCV - V_{cut-off}}{R_{int}} \tag{5-7}$$

As seen from Figure 5.11, the Li-ion battery pack cannot supply enough current to the motor to start the engine, because the starter motor of a vehicle consumes a current around 800-1000A. The Li-ion batteries cannot meet these requirements. As Figure 5.11 shows the maximum current supplied from the battery is around 448A by using the maximum region off the Li-ion battery pack. The maximum current is limited by the voltage of the Li-ion battery pack as seen in the equation (5-7) and the internal temperature.

The information from the graph has been used in the Simulink model to define the boundary conditions; for example the maximum current that can be supplied to the loads at each SOC.

5.2 Combined system

Before building the system in the vehicle, the test of the total combined model is done at the lab bench to investigate the performance. First of all, the model which has been presented in Figure 5.12 is connected. In the first procedure, both batteries are charged to 15.2 V. The system is connected at the lab bench as follows:

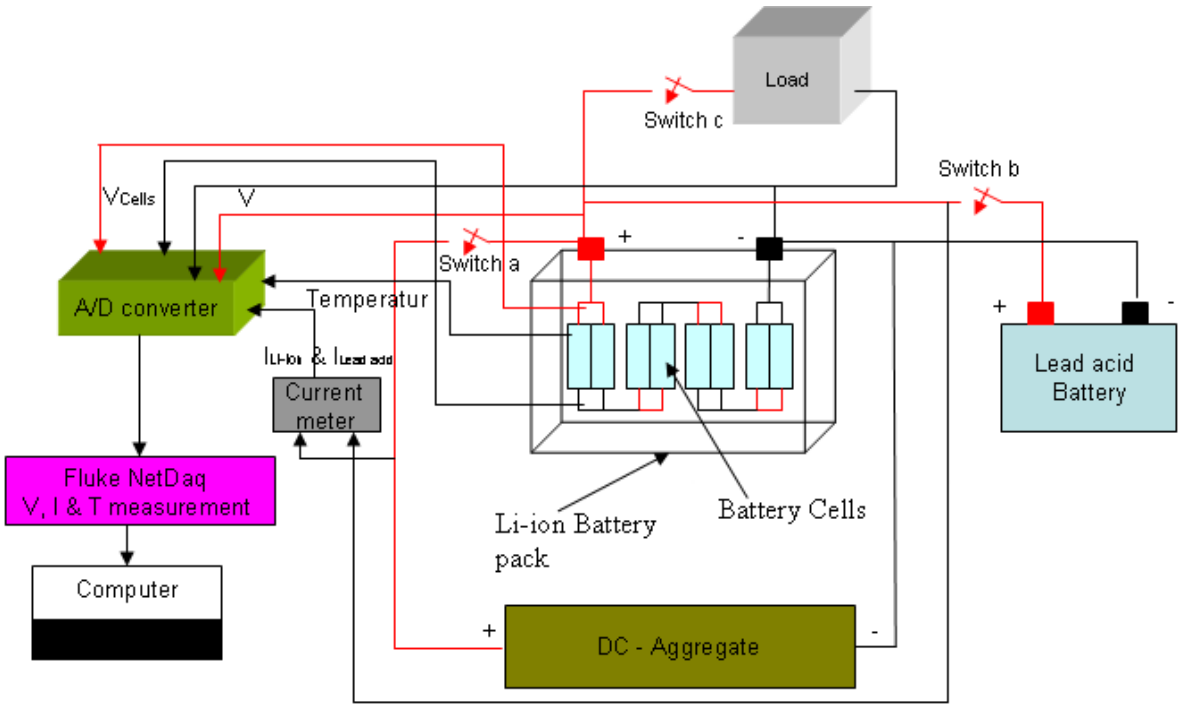


Figure 5.12 The connected model at the lab bench

Figure 5.13 shows a simplified model of the one showed in Figure 5.12.

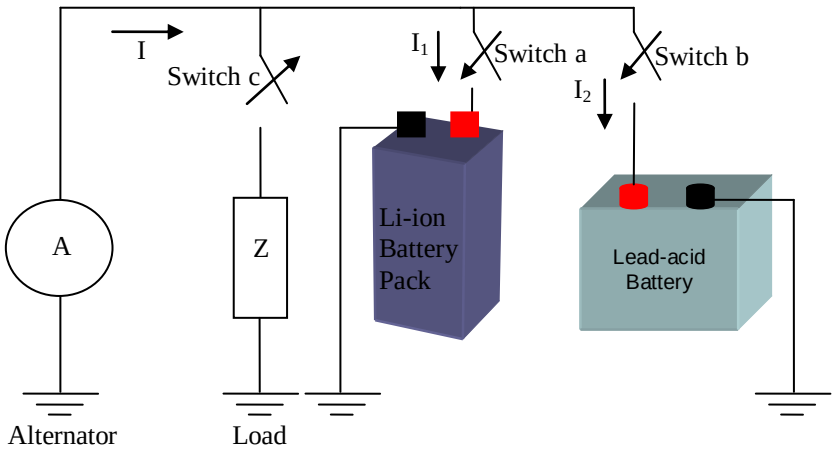


Figure 5.13 The model during charging of the batteries

The loads are disconnected in this case since it is not interesting during charging. When the voltage reaches 15.2V, the alternator (replaced by DC-aggregate in the lab) would stop. The equipments used for measuring the voltage, current and temperature are the same as the instruments used in section 4.1 A.

By the data discussed in Table 1.1 (which are used as assumptions in theoretical and practical applications), the alternator is not able to charge the Li-ion battery to full charge which is 16.6V. Results from testing the Li-ion battery in the first lab is presented in the plot of OCV versus SOC in Figure 5.14.

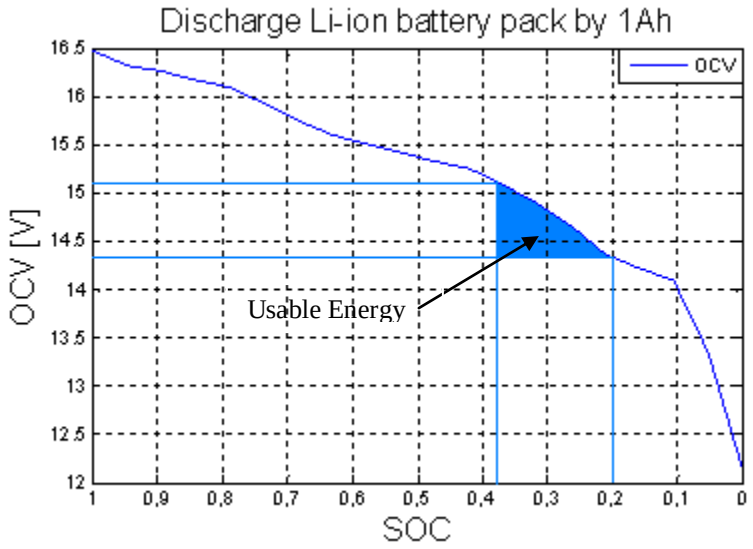


Figure 5.14 Discharge of the Li-ion battery pack with respect to OCV vs SOC, with the total capacity 26.67Ah

As seen from Figure 5.14, the alternator could charge the Li-ion battery up to approximately 39% of SOC. Hence, the working area for the Li-ion battery will be from 39% to the minimum condition of SOC which is 20% of SOC; thus SOC_{usable} is 19% of the total capacity that can be used and that capacity C_{usable} is:

$$C_{usable} = SOC_{usable}\, Q_{tot} = 0.19 \times 26.67Ah = 5A \tag{5-8}$$

This will then yield

$$Ampere - second = C_{usable} \times 1h = 5 \times 3600 = 18242.28As \tag{5-9}$$

Here 1h=3600 seconds, one stop is assumed to be 20s and the loads 50A which leads to

$$\frac{Ampere\ -second}{One\ stop} = \frac{18242.28As}{1000\,As} = 18 \tag{5-10}$$

Therefore, the Li-ion battery can be utilized 18 times before recharging it again to original level in all the cases below.

By comparing the results from the assumptions part and the results in Figure 5.19, the voltage level reaches the limit conditions quicker than what is expected from the calculations. In addition, by calculating as explained above, the battery could discharge approximately 18 times but during the lab it is shown that it could just discharge the Li-ion batteries 8 times. The differences can be contributed to the accuracy error in the lab, the aging mechanisms inside the battery and also the voltage loss through the cables.

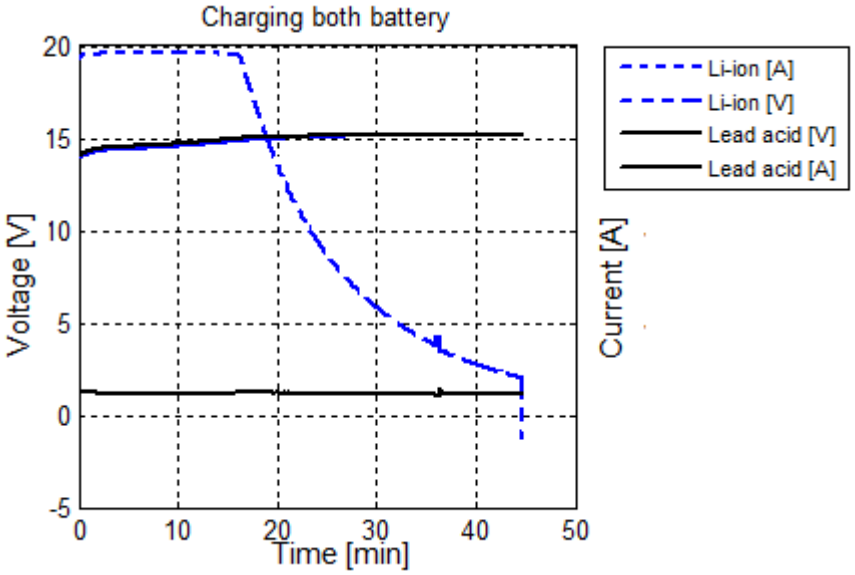


Figure 5.15 The current and voltage over both battery packs during charge

As from the Figure 5.15, the current flow is higher through the Li-ion battery than the lead-acid battery because the input voltage exceeds that of the threshold voltage and the lead-acid battery is fully charged at 12.9V. This model explained the fact that the battery system can work when the lead-acid battery suffers overcharge. From the figure, the voltage goes over the threshold but the current flow is low in the lead-acid battery. Under the overcharge situation, the aging mechanism inside the lead-acid battery is pretty serious, so the internal resistance of the lead-acid battery increases very quickly as discussed in chapter 2.

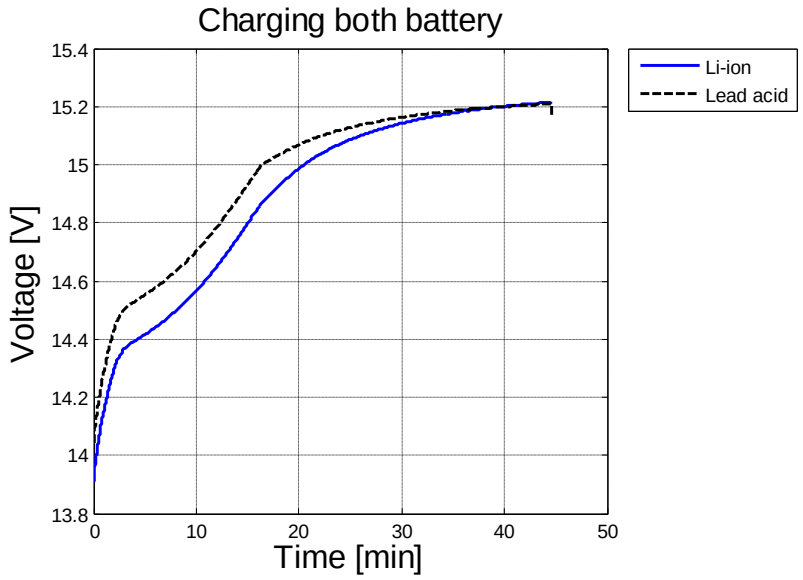


Figure 5.16 The voltage versus time during charging of the combined system

From Figure 5.16, the voltage increase per unit of lead-acid battery is higher than that of lithium ion battery. Because in this situation, the lead-acid battery has already been fully charged and now is overcharging, the current passing through the lead-acid battery is nearly zero; therefore, the voltage increase is just directly induced by the electric force which is produced by the voltage from the alternator.

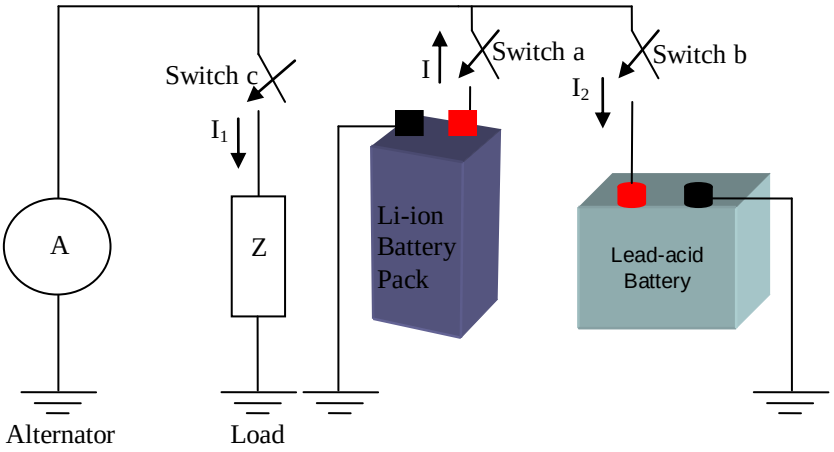


Figure 5.17 The first model during discharge of the batteries

The discharge of the batteries is done by disconnecting the alternator, while the current variable load is set to 50A and turned on for spans of approximately 20 sec and off for a few minutes, to compare the times the Li-ion battery pack could be utilized before it needs to be charged to 15.2 V again. The interesting notion of this test is to see if the Li-ion battery will charge the lead-acid battery as well or whether the lead-acid discharges during stop time.

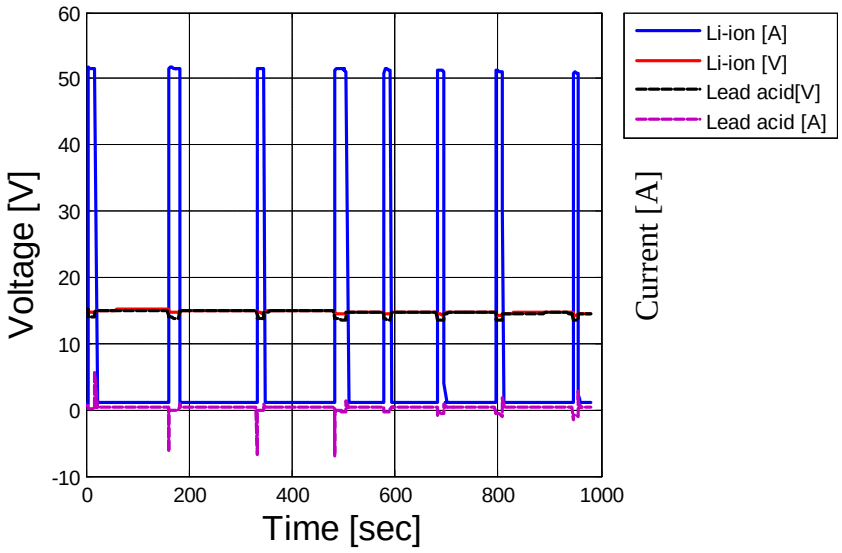


Figure 5.18 Measured voltage and current versus time during the stops

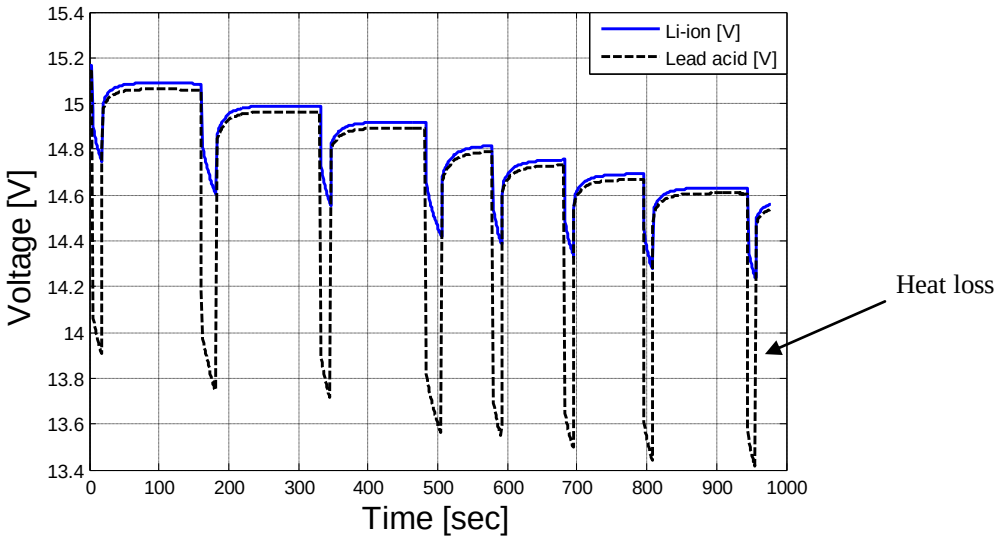


Figure 5.19 The terminal voltages over both batteries

Figures 5.18 and 5.19 visualize the fact that when the load is on, it caused higher voltage drops over the Li-ion battery, and all current is supplied from the Li-ion battery pack to the load. After eight stops, the Li-ion battery reaches the used region which is around 14.2 V as explained before. When the load is off, the voltage of the lead-acid battery increases and very small current flows through and charges the lead-acid battery as discussed before. Those current flows can be neglected but after many repetitions this will lead to quicker discharge of the Li-ion battery and overcharge of the lead-acid battery pack which affects the ageing of the batteries. To prevent that small currents flow from the Li-ion to the lead-acid battery, a diode can be connected in parallel with a switch and series in front of the lead-acid battery pack as explained before.

If the lead-acid battery is not fully charged, using this system would lead to the lead-acid battery being charged by the Li-ion for every stop cycle. As mentioned before, by including a diode, this problem would be solved. A benefit of this model is that by keeping the lead-acid battery fully charged, the charging of the lead-acid battery by the Li-ion battery pack can be prevented during the stop time. It provides a cheap solution by using less power electronics which increase the safety of the vehicle since electronics can break down or be damaged.

As seen from Figure 5.19, when the load is on, the voltage of lead-acid battery drops by 0.8V.

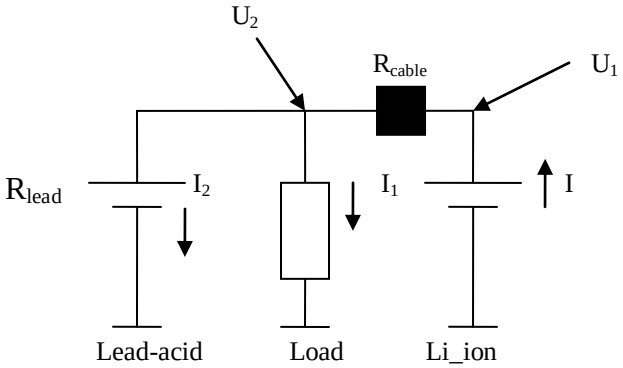


Figure 5.20 The combined system during discharging

This is due to the heat loss of lead-acid battery and the cable between these two batteries. The voltage over the load can be calculated as.

$$(U_1 - U_2)It = {I_2}^2 R_{lead}\, t + I^2 R_{cable}\, t \qquad (5\text{-}11)$$

This phenomenon should be taken into consideration when dealing with the tests explained further on.

Figures 5.21 and 5.22 below show the charge/discharge voltage and currents over the batteries for one cycle of stop for approximately 20 sec. The load is set to 50A and a constant voltage (CV) is used for charging time repeatedly.

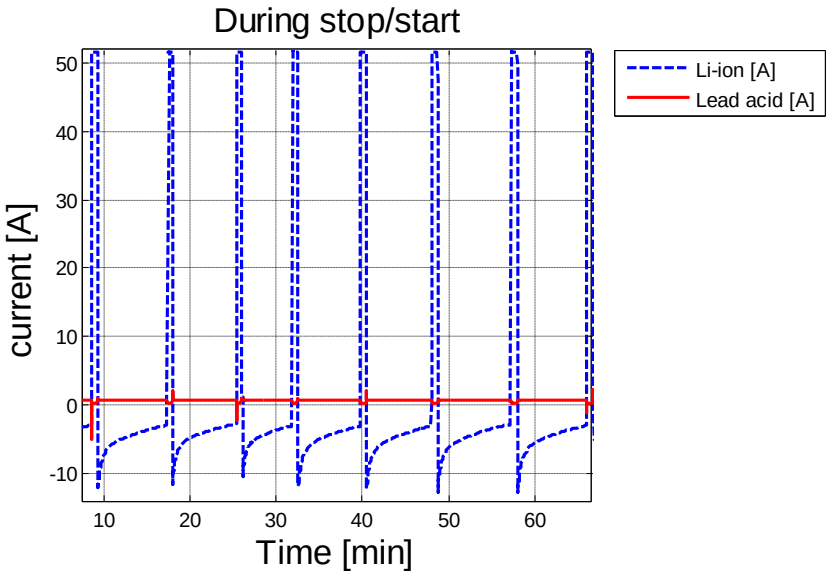


Figure 5.21 The in/out put current through both battery packs during stop/start time, CV (negative values mean charging current)

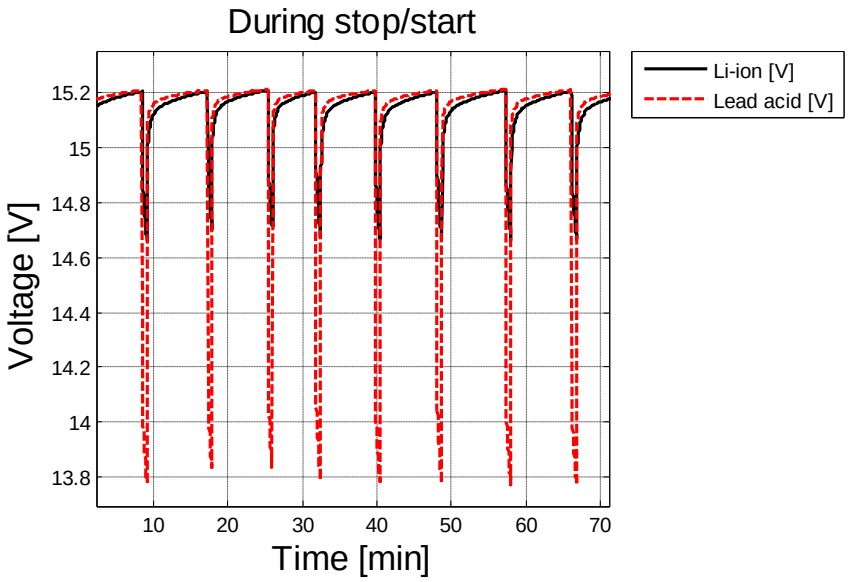


Figure 5.22 The terminal voltage over both battery packs during stop/start time, CV

Comparing the two situations discussed above, if the battery system is discharged in the second situation (discharging the battery from 15.2V until it reaches 14.2V and recharging it to the original level), it would spend much more time to charge the battery system, while the energy output from the first case can match the requirements in this work. Therefore, the solution which will charge the battery system directly after discharging is chosen.

Figure 5.23 shows the voltages and currents over the battery packs during charge/discharge by constant current charging system (CC).

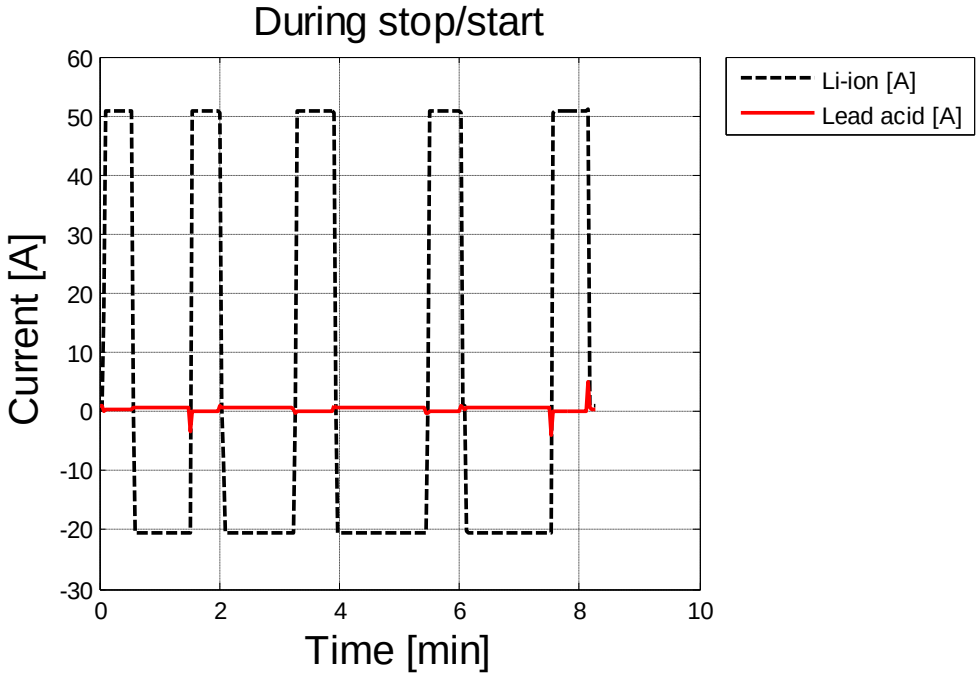


Figure 5.23 The in/output current through both battery packs during charge and discharge time, CC

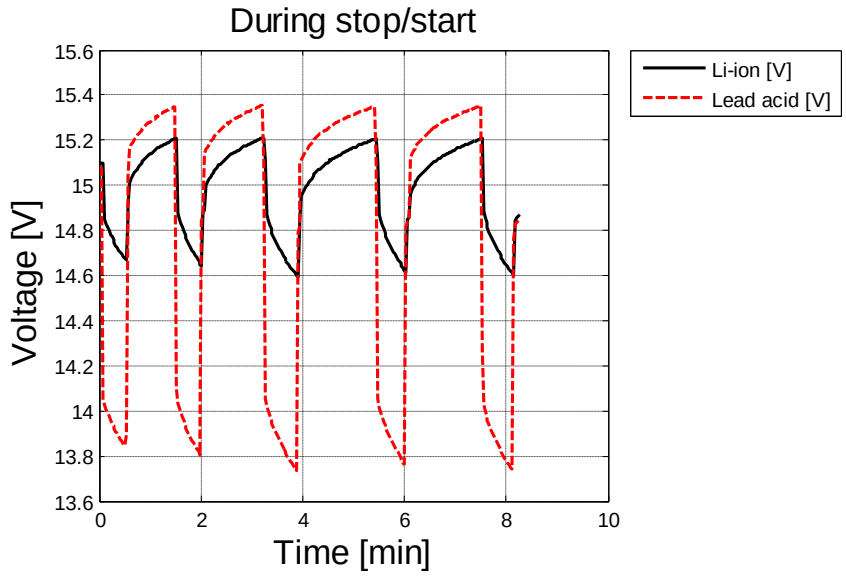


Figure 5.24 The thermal voltage over both battery packs during charge and discharge time, CC

Figures 5.23 and 5.24 above show that using CC would lead to much quicker charging of the Li-ion battery; in the CV case it takes around 10 minutes while the CC takes around 1 minute. However, the temperature increase would be more in CC than in CV, thus, the energy loss in CC charging is higher than that in CV. Therefore, CV charging method would be chosen in the future tests.

According to the investigations and conclusions above, the following tests of the combined system will be performed in order to get a more reasonable voltage range which will be the boundary conditions in the control model. Figures 5.25 and 5.26 describe the voltage range between 15V and 14.2V, while Figure 5.27 and 5.28 depict the voltage range between 15V and 14.6V.

From the figures below, these two voltage ranges both match the requirements. Apparently, the former ΔV_1 is double as large as the latter ΔV_2, the charging time will be proportionally larger. However, by considering the reality in the vehicle, the maximum voltage supplied by the alternator is nearly 14.8V. And by obeying the requirements of maximum energy output in the reasonable range in case of some accidents, the voltage range between 14.8V and 14.2V is finally defined in this work.

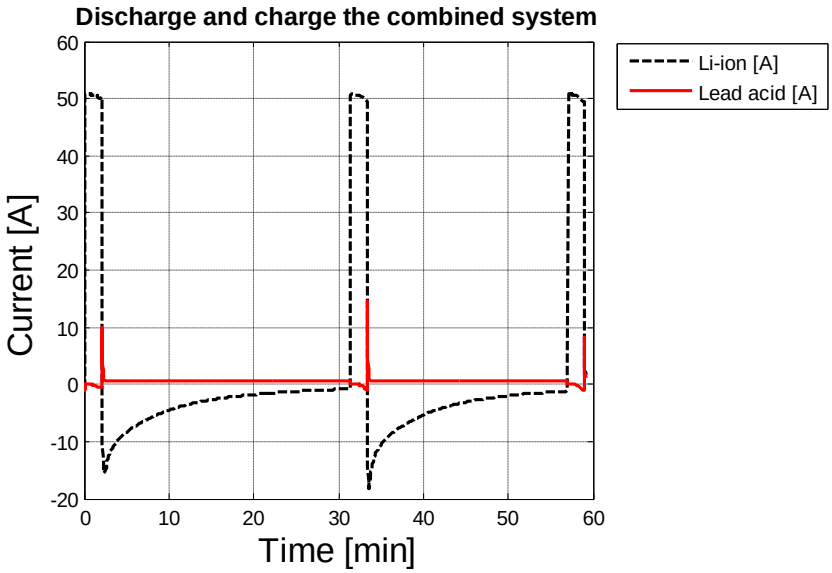


Figure 5.25 Measured currents versus time in the voltage range between 15V and 14.2V

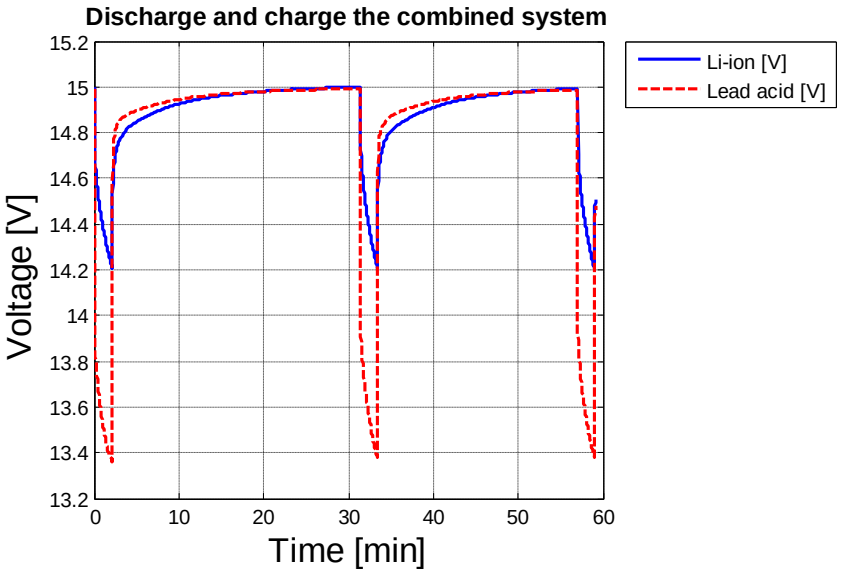


Figure 5.26 Measured voltages versus time in the voltage range between 15V and 14.2V

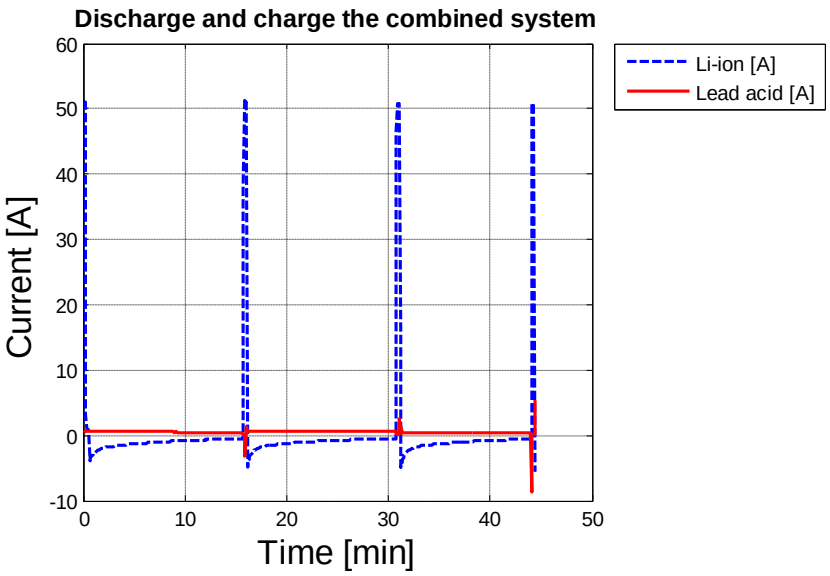


Figure 5.27 Measured currents versus time in the voltage range between 15V and 14.6V

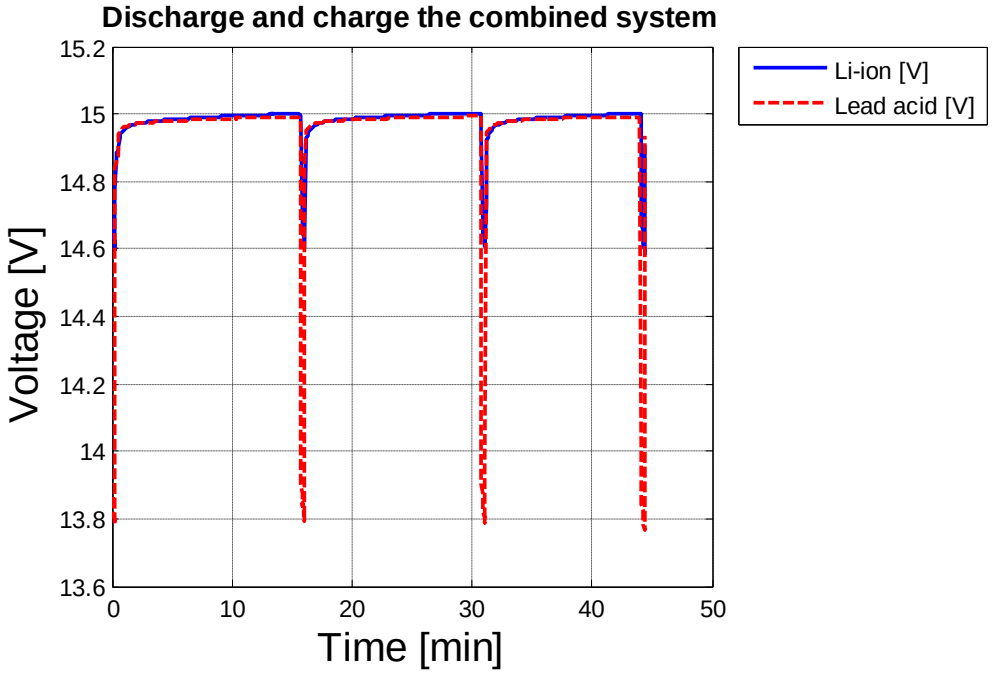


Figure 5.28 Measured voltages versus time in the voltage range between 15V and 14.6V

5.3 Verification in vehicle

Based on the experiments discussed above, the working area for the Li-ion battery will be approximately between 35% - 20% SOC. By the same assumptions as Table 1.1, where one stop is 20s, with 15% SOC_{usable} and using the equations 5-10 to 5-12 yields 14 discharge times of the Li-ion battery pack before charging it again.

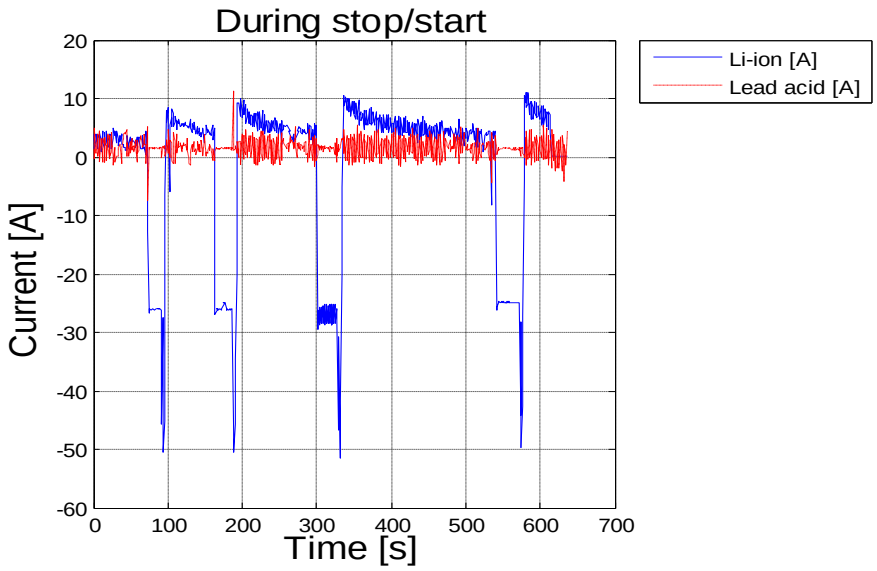


Figure 5.29 The current flow for both battery packs in the vehicle

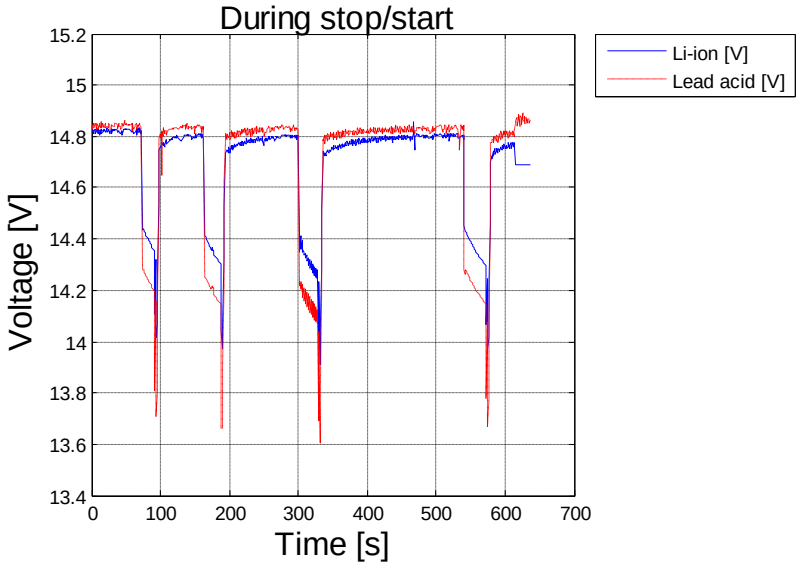


Figure5.30 The voltage versus time for both batteries pack in the vehicle

Keeping the output voltage of the alternator on 14.9V was not possible, because the voltage of alternator is not sufficiently stable and due to the lead-acid battery's temperature. Figures 5.29 and 5.30 show where the voltage level from the alternator could be kept at 14.8V for just some cycles, and it works without any problems. Thus, as seen from Figures 5.30 and 5.31, the Li-ion battery supplies the loads during the stops as expected.

The processing region for the Li-ion battery will be less than what has been assumed which is slightly above 14.6V, because the alternator output voltage could not be kept stable at 14.8V. In that area of the Li-ion battery the voltage is sensitive and can drop very quickly. Therefore, after every stop the battery must be charged again to the target value of the voltage level as Figure 5.31 shows. The driving distance in the test was rather short.

The following Figures 5.32 and 5.33 are repeated tests as above but with the different driving time and lower alternator output voltage. The system can be implemented successfully in the vehicle.

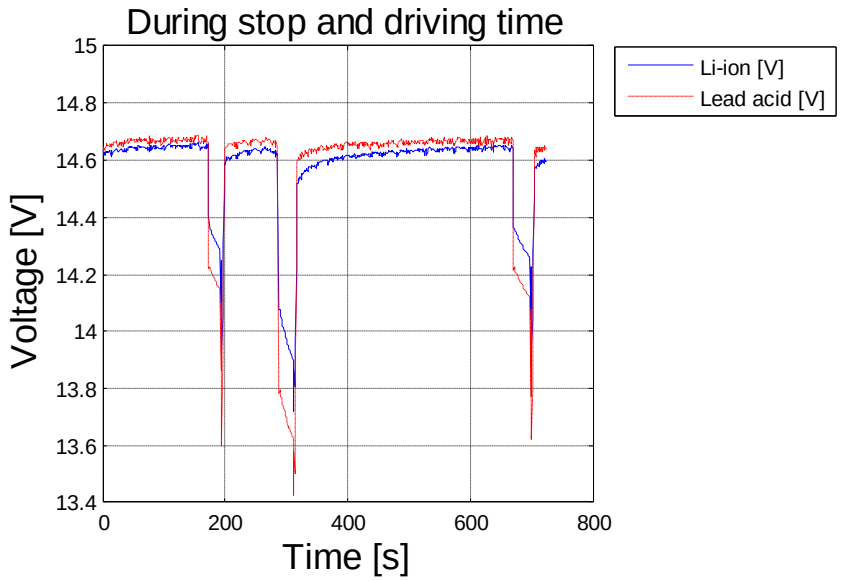


Figure 5.31 Measured voltages versus time from the tests in the vehicle

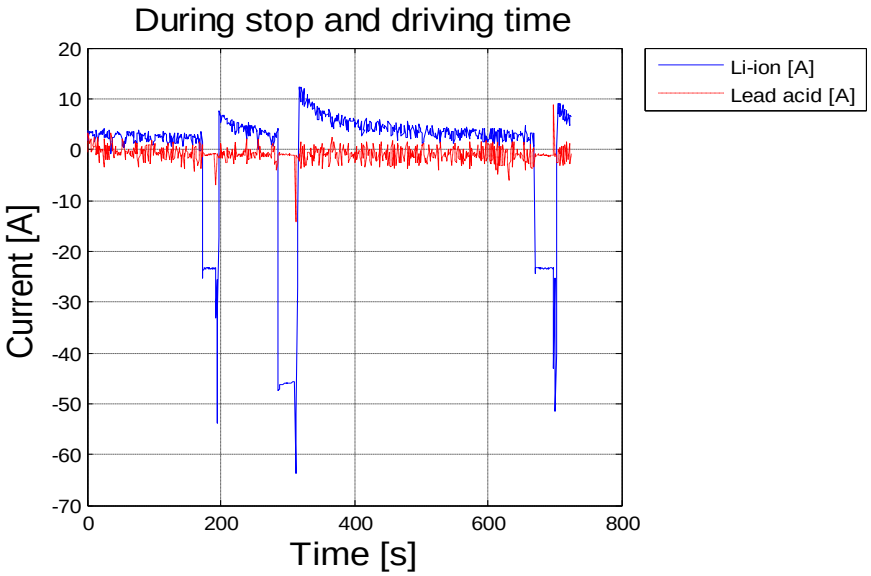


Figure 5.32 Measured currents versus time from the tests in the vehicle

The following Figures 5.33 and 5.34 show how the charge/discharge controller is processing.

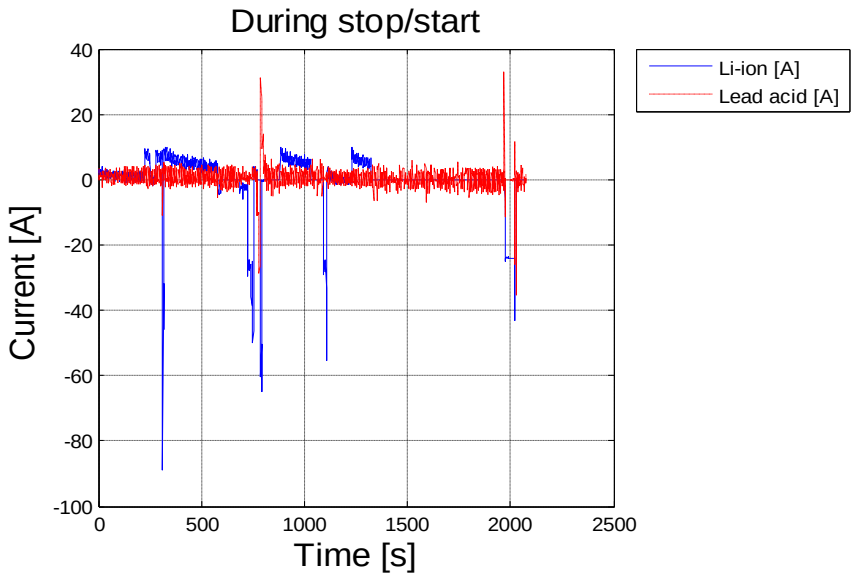


Figure 5.33 Measured currents versus time from repeated tests in the vehicle

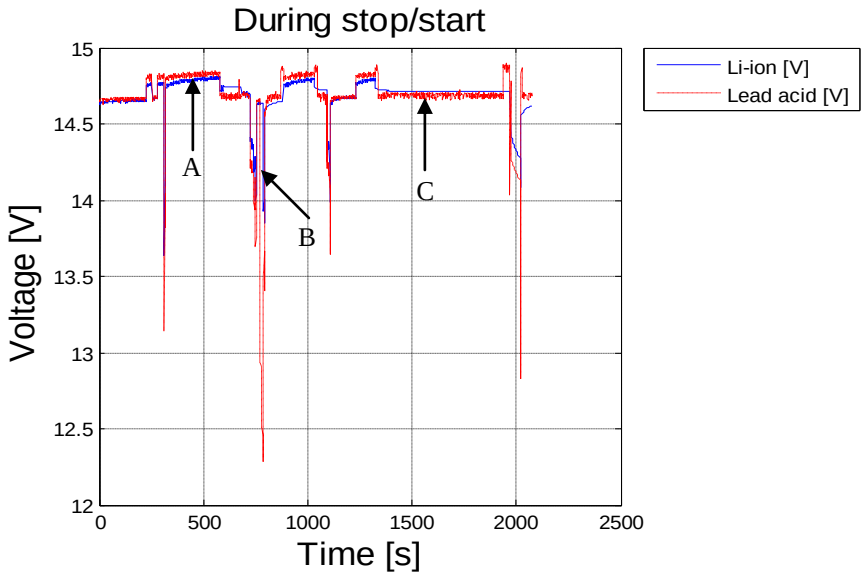


Figure 5.34 Measured voltage versus time from repeated tests in the vehicle

In region A the relay is on to charge the Li-ion battery after every discharge, B is on for discharge and at the region C the relay is off because the SOC of Li-ion battery pack has reached the target level and is ready to be discharged again. Thus the controller system works as expected (more information and detail about the controller system is presented in the appendix A).

6. Conclusions

The work summarized in this thesis has investigated the behavior of different dual battery solutions, which could be used for the start-stop application in vehicles. Some tests have been conducted on the Li-ion battery in parallel with the lead-acid main battery. The controller system for this battery system has been simulated in Simulink to control the charge and discharge processes.

The interesting conclusion with this work was that a cheap and simple system solution was verified and tested successfully in the vehicle. The system solution shows promising performance of how the controller system works and that during the stop time, only the Li-ion battery is supplying the power to the loads in the vehicle. However, one drawback is the fact that the lead-acid battery would be charged slightly during stop time by Li-ion battery. This small current can be neglected, but it could in the future lead to a decrease in the life time due to overcharge. An improvement to this can be the system solution B in which a diode is installed to prevent the currents to flow from the Li-ion battery to the lead-acid battery. And the price of system solution B can be accepted from the economical point, so this solution would be a nice choice and can be performed and verified in the future. The Simulink model could serve as a basis for further improvements to this system.

Meanwhile, the performance of the Li-ion battery satisfies the requirements, which can be seen from the data we tested. Due to the time limitation of this work, more monitoring measurement and verifications should be performed continually for long-term effects. If the working voltage ranges of a new Li-ion battery can be closer to that of the lead-acid battery, so the system solution can be easy and cheap by using less electronics. This will be discussed in the next chapter.

7. Outlook

By considering the requirements discussed above, it would be better to use another lithium ion battery to match the requirements in this work. This should have the same voltage levels as the lead-acid battery, but a higher capacity range to utilize. If so, it would not need a DC/DC converter and an advanced controller system. This would cost less and be easier to use. The characteristics of the lithium ion battery expected in this case should match the rough graph in Figure 7.1. Compared with the energy storage discussed in chapter 2, the potential lithium ion battery technology for start-stop application is based on e.g. olivine framework $LiFePO_4$ cathodes.

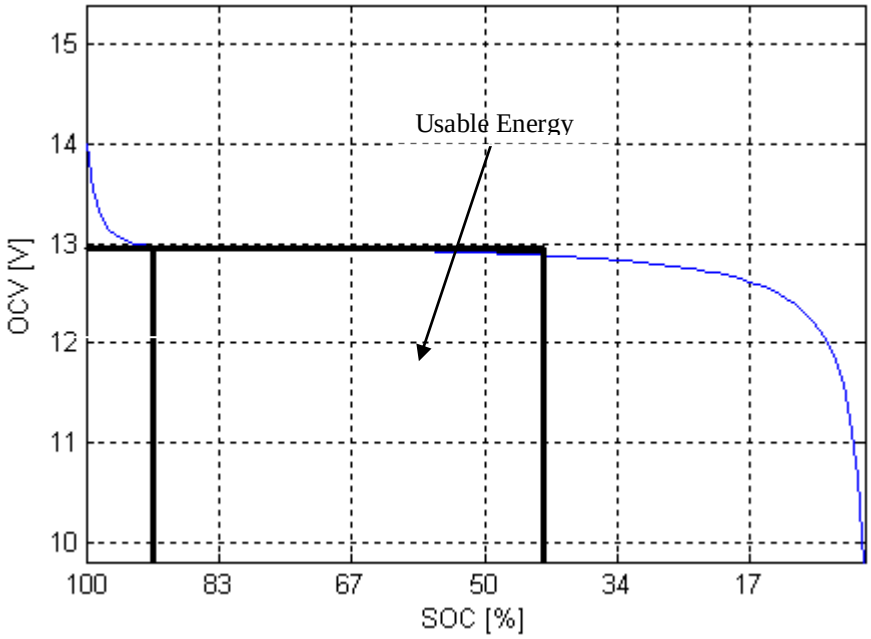


Figure 7.1 OCV versus SOC for the future battery type.

In the future, if this new type of lithium ion battery would be used in the start-stop application, the control model and the boundary conditions should be easier than the one discussed here. The estimation of the whole scope, considering the performance and the cost, could match the economy requirements in the industry.

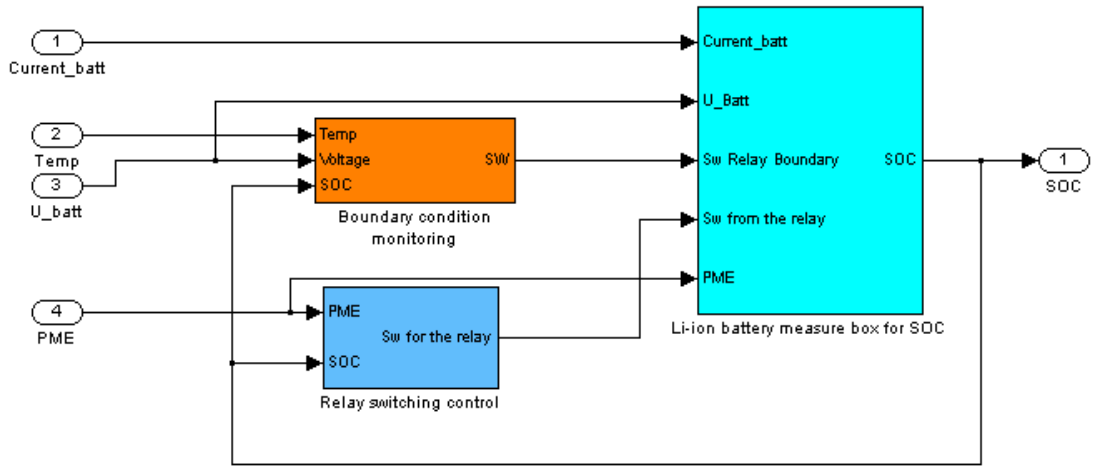
Some future work can be done by using one of the same system solutions as presented in this thesis and use $LiFePO_4$ instead for the one which has been used here. Since the $LiFePO_4$ has a much higher usable energy amount, as seen from Figure 7.1, it can be used for a free roll system in vehicle. Free roll system means that the engine can shut down when the vehicle is in driving mode and has kinetic energy i.e. down-hill driving. In this case, the electronic equipment will increase and require more power from the battery pack.

8. References

1. JB Goodenough. Positive electrode: Layered Metal Oxides (2009). Elsevier B.V.
2. Elton J.Cairns. Batteries, Overview (2004). Encyclopedia of Energy. Vol1.
3. D.A.J.Rand et al. Valve-Regulated Lead-Acid Batteries (2004). Elsevier B.V.
4. J Albers, et al., Lead-acid batteries in micro-hybrid vehicles. J. Power Source (2010), doi: 10.1016/j.jpowsour.2010.11.094
5. Masataka Wakihara. Recent developments in lithium ion batteries. Materials Science and Engineering R33(2001) 109-134
6. J.Vetter. Ageing mechanisms in lithium ion batteries. J. Power Source 147(2005)269-281
7. http://www.mpoweruk.com/chemistries.htm 2011-02-18 entry
8. M.Wakihara. Lithium-ion batteries: fundamentals and performance
9. http://batteryuniversity.com/learn/article/how_does_internal_resistance_affect_performance 2011-03-15 entry
10. Yuichi Sato. Cause of the memory effect observed in alkaline secondary batteries using nickel electrode. J. of Power Sources 93(2001)20-24
11. Elisabet Ahlberg. Capacity loss in Ni-Cd pocket plate batteries. The origin of the second voltage plateau. J of Power Source 85(2000)245-253
12. http://www.mpoweruk.com/life.htm 2011-03-20 entry
13. http://www.mpoweruk.com/thermal.htm 2011-03-20entry
14. Minoru Inaba etc. Up-to-date Development of Lithium-ion Batteries in Japan. IEEE Electrical Insulation Magazine
15. http://www.mpoweruk.com/bms.htm battery management system 2011-05-20 entry
16. Daniel. D Friel. Management of Batteries for Electric Traction Vehicle. USA (2010) Elsevier B.V.
17. Dennis Doerffel et, all. Large Lithium-Ion Batteries – a Review. UK (2006)
18. http://www.mpoweruk.com/soc.htm 2011-05-30 entry
19. Jie Xu et, all. Design and Study on the State of Charge Estimation for Lithium-ion Battery Pack in Electric Vehicle. China (2009) IEEE computer society
20. Amir M. Rahimi. A Lithium-Ion Battery Charger for Charging up to Eight Cells. USA 7-9 Sept. 2005 IEEE
21. http://www.mpoweruk.com/chargers.htm 2011-03-10 entry
22. http://en.wikipedia.org/wiki/Schottky_diode 2011-05-20 entry

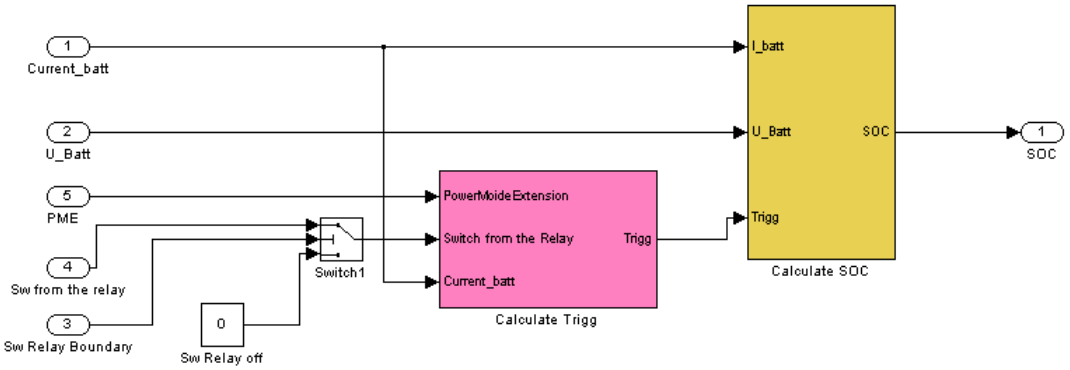
Appendix A

Simulink model

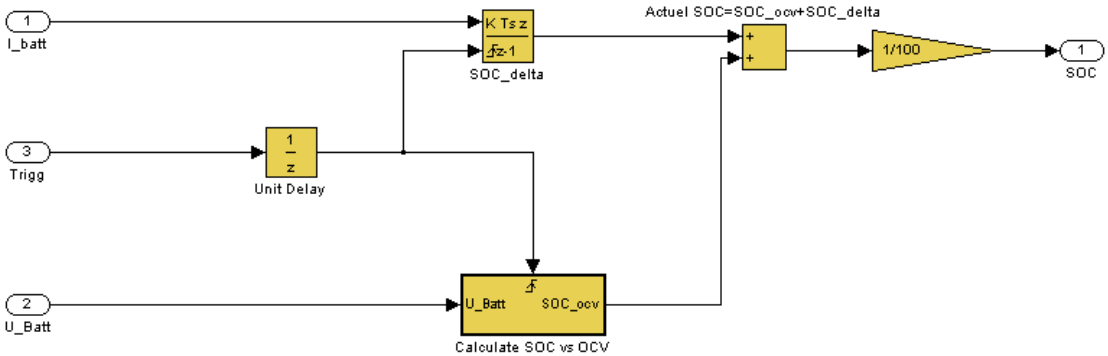


Appendix A figure1. The main Simulink model

The controller system is decided by the following input and output signals as presented in appendix figure1.

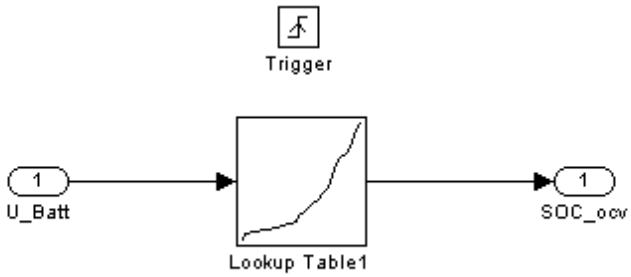


Appendix A figure2. The Li-ion battery measure-box for the SOC block

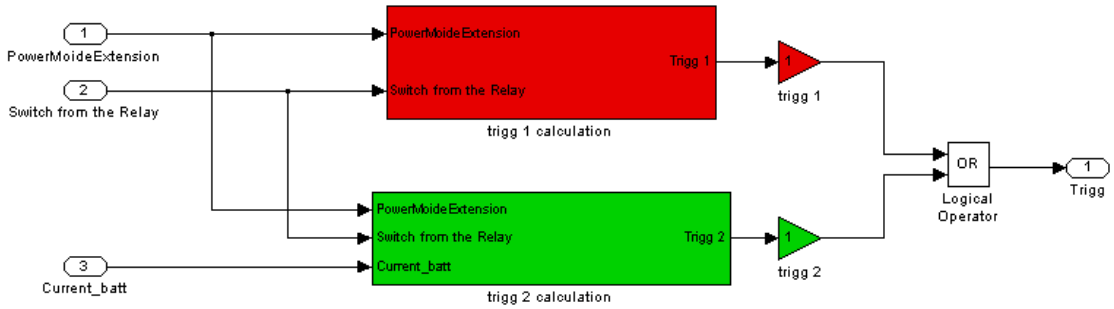


Appendix A figure3. The Li-ion battery measure box for the SOC block

By measuring the current, the ΔSOC can be calculated; by getting the correct trigger from calculations at the right instance and by measuring the battery voltage, SOC_{OCV} can be obtained.



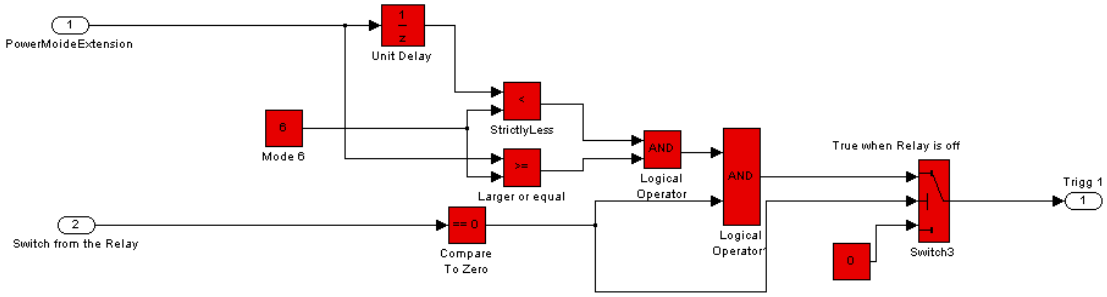
Appendix A figure4. The SOCocv calculation block



Appendix A figure5. Block for calculating trigger

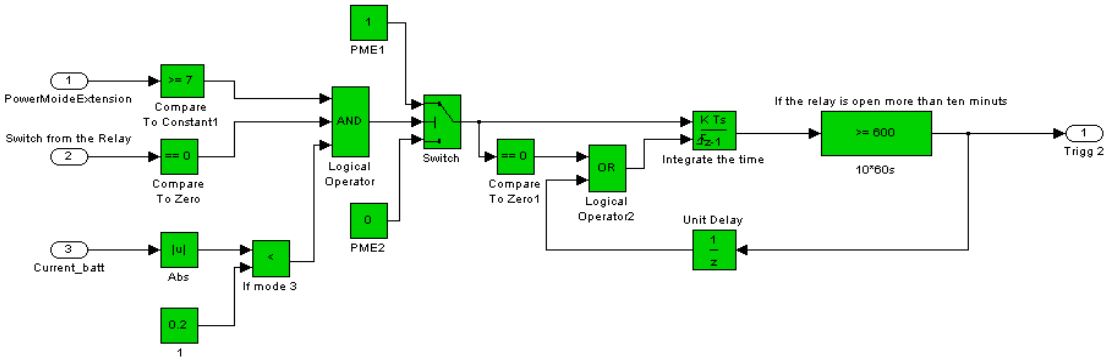
The Power Mode Extension (PME) signal includes ten different signals from 0-9 which corresponds to the three key positions of the vehicle; 0-5 correspond to position 0, 6 is position 1; that is ignition but the engine is off, while 7-9 are position 2. For the value 7 the engine is on, for 8 the engine is off in standby and in 9 the engine will start again. By knowing those input signals, the controlling of the Li-ion battery pack and Relay A will be decided to whether charge or discharge the Li-ion battery.

Corresponding to those signals, the switching of relay A is decided.



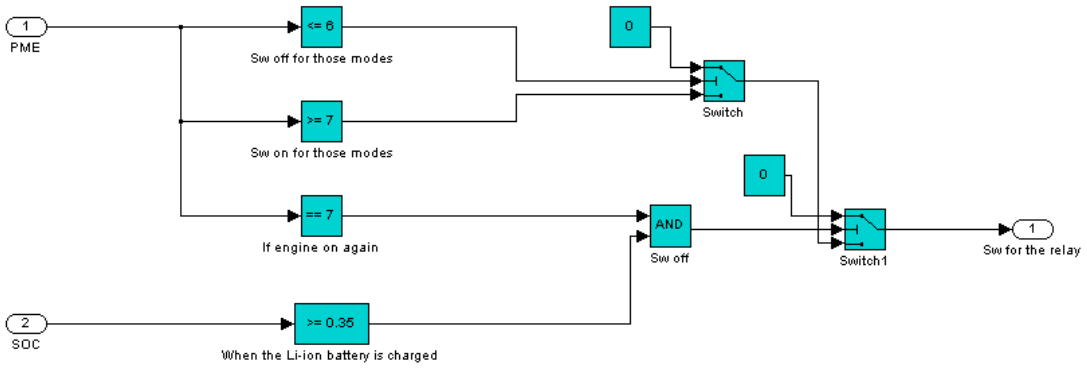
Appendix A figure6. Block for determining trigger A

The trigger determines when SOC_{OCV} will be calculated. The first trigger will occur when mode 6 is activated and relay A is off.



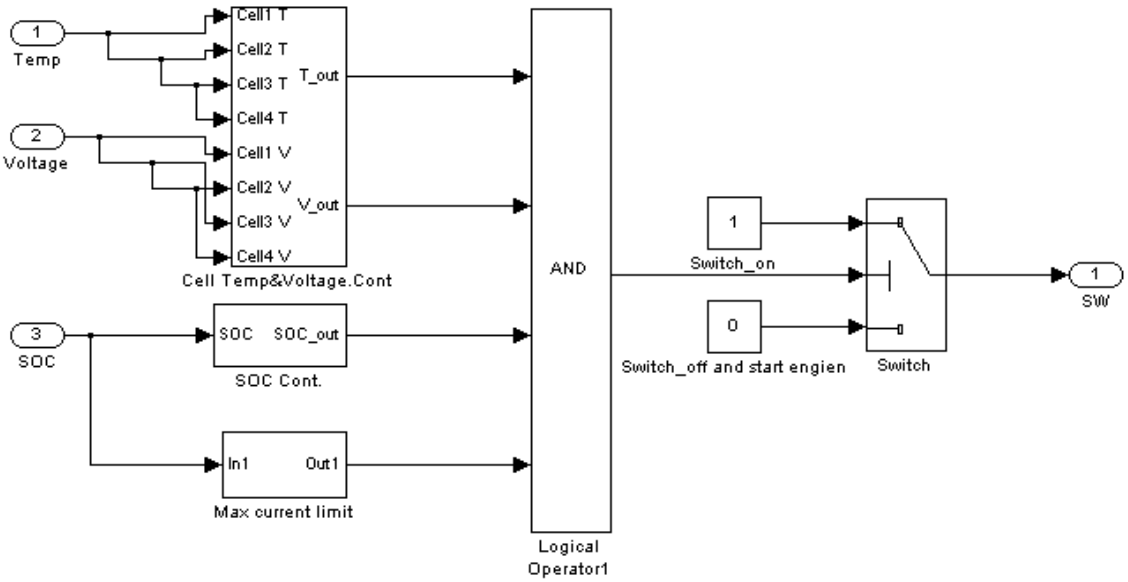
Appendix A figure7. Block for calculating trigger 2

The second trigger will occur when the PME is larger or equal to seven, relay A is off and the current flowing from the battery pack is close to zero. Then it will give a new calculation of SOC_{OCV}; if relay A is off more than ten minutes, which is 600s (this time could be less than ten minutes to get more updating SOC value), the new SOC_{OCV} will be calculated rapidly.

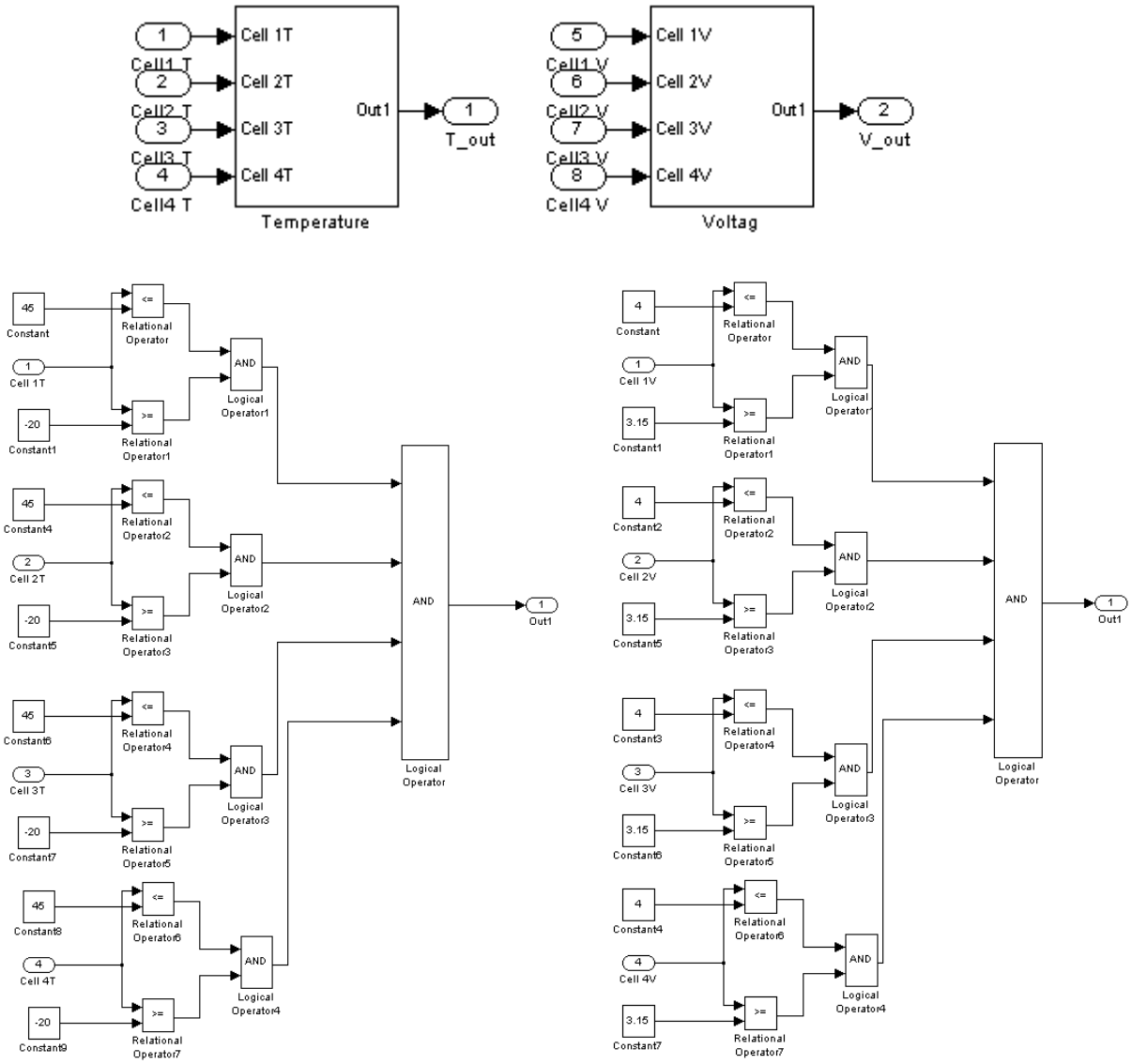


Appendix A figure8. The relay A switching control block

By inputting the PME and the battery voltage, the switching controller is decided. Thus, relay A is open when the PME is between 7-9 and when the SOC over the battery pack reaches 0.35 (35%) the relay should be off since the battery is charged.

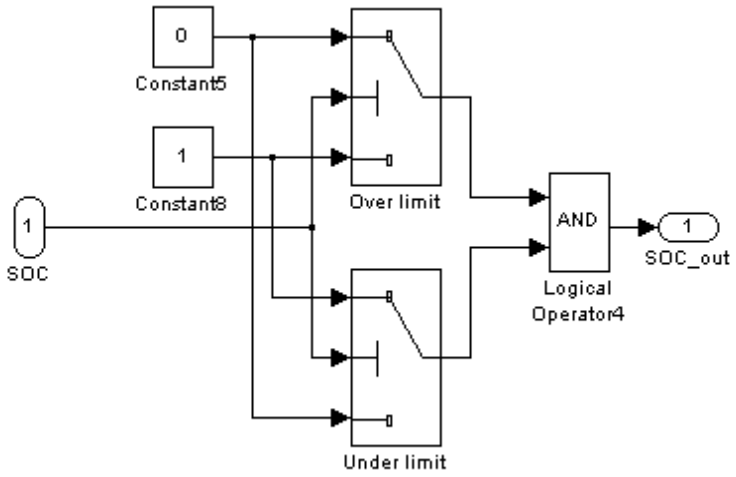


Appendix A figure9. The boundary condition for the monitoring block



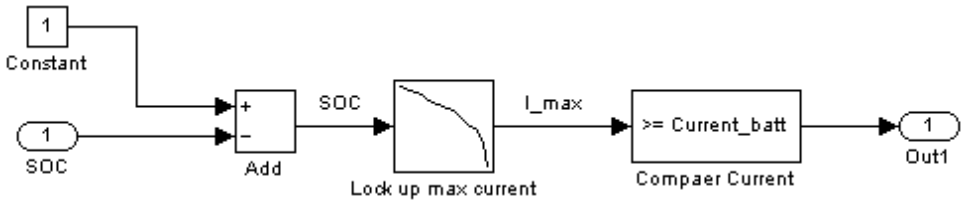
Appendix A figure10. The temperature & voltage conditions block

The temperature and voltage monitoring is done for each cell, but during the test in the vehicle it is assumed for one cell's temperature and the total voltage over the battery pack.



Appendix A figure11. The SOC control block

The SOC control is between the working area of the battery limitation. In this project the SOC should not proceed above 39% and below 20%.



Appendix A figure12. The max current limit block

By knowing the SOC of the battery its corresponding max current could be able to be produced. The I_{max} must be higher than the battery current flow, otherwise the switch will be off.

In all cases for the boundary conditions, relay A must be interrupted from the circuit if one of the parameters exceeds the limitation area.